

Article

The RNA Helicase Ded1 from Yeast Is Associated with the Signal Recognition Particle and Is Regulated by SRP21

Hilal Yeter-Alat ^{1,2}, Naïma Belgareh-Touzé ³, Agnès Le Saux ^{1,2}, Emmeline Huvelle ^{1,2}, Molka Mokdadi ^{1,2,4,5}, Josette Banroques ^{1,2} and N. Kyle Tanner ^{1,2,*} 

¹ Expression Génétique Microbienne, UMR8261 CNRS, Université de Paris, 13 rue Pierre et Marie Curie, 75005 Paris, France; yeter.hilal@yahoo.fr (H.Y.-A.); lesauxagnes@yahoo.fr (A.L.S.); emmeline.huvelle@i2bc.paris-saclay.fr (E.H.); molka.mokdadi@gmail.com (M.M.); josette.banroques@ibpc.fr (J.B.)

² Expression Génétique Microbienne, Institut de Biologie Physico-Chimique, Paris Sciences et Lettres University, 75005 Paris, France

³ Laboratoire de Biologie Moléculaire et Cellulaire des Eucaryotes, UMR8226 CNRS, Sorbonne Université, 13 rue Pierre et Marie Curie, 75005 Paris, France; naima.belgareh@ibpc.fr

⁴ Laboratory of Molecular Epidemiology and Experimental Pathology, LR16IPT04, Institut Pasteur de Tunis, Université de Tunis El Manar, Tunis 1002, Tunisia

⁵ Institut National des Sciences Appliquées et Technologies, Université de Carthage, Tunis 1080, Tunisia

* Correspondence: kyle.tanner@ibpc.fr; Tel.: +33-1-58-41-52-37

Abstract: The DEAD-box RNA helicase Ded1 is an essential yeast protein involved in translation initiation that belongs to the DDX3 subfamily. The purified Ded1 protein is an ATP-dependent RNA-binding protein and an RNA-dependent ATPase, but it was previously found to lack substrate specificity and enzymatic regulation. Here we demonstrate through yeast genetics, yeast extract pull-down experiments, in situ localization, and in vitro biochemical approaches that Ded1 is associated with, and regulated by, the signal recognition particle (SRP), which is a universally conserved ribonucleoprotein complex required for the co-translational translocation of polypeptides into the endoplasmic reticulum lumen and membrane. Ded1 is physically associated with SRP components in vivo and in vitro. Ded1 is genetically linked with SRP proteins. Finally, the enzymatic activity of Ded1 is inhibited by SRP21 in the presence of SCR1 RNA. We propose a model where Ded1 actively participates in the translocation of proteins during translation. Our results provide a new understanding of the role of Ded1 during translation.

Keywords: DEAD-box; Ded1; DDX3; SCR1; SRP; translocon; ATPase; Sec61; translation



Citation: Yeter-Alat, H.; Belgareh-Touzé, N.; Le Saux, A.; Huvelle, E.; Mokdadi, M.; Banroques, J.; Tanner, N.K. The RNA Helicase Ded1 from Yeast Is Associated with the Signal Recognition Particle and Is Regulated by SRP21. *Molecules* **2024**, *29*, 2944. <https://doi.org/10.3390/molecules29122944>

Academic Editor: Leonidas A. Phylactou

Received: 22 May 2024
Revised: 12 June 2024
Accepted: 18 June 2024
Published: 20 June 2024



Copyright: © 2024 by the authors. Licensee MDPI, Basel, Switzerland. This article is an open access article distributed under the terms and conditions of the Creative Commons Attribution (CC BY) license (<https://creativecommons.org/licenses/by/4.0/>).

1. Introduction

The DEAD-box family of RNA helicases are ubiquitous proteins found in all kingdoms of life, and they are implicated in all processes involving RNA, from transcription, splicing, ribosomal biogenesis, RNA export, and translation, to RNA decay (reviewed in [1–3]). They belong to the DEXD/H superfamily 2 (SF2) of putative RNA and DNA helicases that contain catalytic cores consisting of two linked RecA-like domains containing conserved motifs associated with ligand binding and NTPase activity, where the majority of the proteins are ATPases. In addition, they often contain highly variable amino- and carboxyl-terminal domains (reviewed in [4,5]). The DEAD-box proteins are ATP-dependent RNA-binding proteins and RNA-dependent ATPases that have been shown to remodel RNA and ribonucleoprotein (RNP) complexes and to unwind short RNA duplexes in vitro, but they are not processive, and they generally have shown little to no substrate specificity [1–3]. However, recent single-molecule studies of the DEAD-box protein Ded1 indicate that these properties may be secondary to their ability to form ATP-dependent clamps on RNA [6].

A number of crystal structures of DEAD-box proteins have been solved in the presence and absence of ligands (reviewed in [7]). In the absence of ATP, the two RecA-like domains

are unconstrained (“open” conformation), and the proteins have low affinity for RNA. In the presence of ATP, the two RecA-like domains are highly constrained (“closed” conformation) and have a high affinity for the RNA. RecA-like domain 2 binds the 5′ end of the RNA in the form of an A helix, which can be single- or double-stranded. In contrast, RecA-like domain 1 binds the 3′ end of the RNA with a kink as a result of steric hindrance from residues from motifs Ib and GG, which is incompatible with a duplex. This is not only considered the mechanism for the duplex unwinding activity but it also effectively locks the protein onto the RNA and prevents sliding. Indeed, Ded1 in the presence of the nonhydrolyzable ATP analog ADP-BeF_x forms long-lived complexes on RNA in vitro [8].

Ded1 is a budding-yeast DEAD-box protein that is the functional homolog of mammalian DDX3 (reviewed in [9–12]). It is an essential gene in *Saccharomyces cerevisiae* that can be rescued by the expression of its orthologs from other eukaryotes, including human DDX3 ([13] and references therein). Thus, the functional activity of Ded1 is conserved in eukaryotes. Ded1 is considered a general translation-initiation factor that is important for 48S pre-initiation complex (PIC) scanning to the initiation codon and the formation of the 48S initiation complex (IC) at the AUG codon ([14–16] and references therein). We have shown that Ded1 is a cap-associated factor that actively shuttles between the nucleus and cytoplasm using both the XpoI/Crm1 and Mex67/TAP nuclear pore complexes [13]. Moreover, it interacts with both the nuclear and cytoplasmic 3′ polyA-binding proteins Nab2 and Pab1, respectively. We found that these cap-associated factors stimulate the RNA-dependent ATPase activity of Ded1 [13]. The activity of Ded1 is also modulated by Gle1 and by the Xpo1-Ran[GTP] complex [13,17,18]. Other work has shown that Ded1 is sequestered in cytoplasmic foci (P-bodies or stress granules) with translation-inactive mRNAs during conditions of stress (reviewed in [19–22]). Human DDX3 has similar properties (reviewed in [23]).

We are interested in a better understanding of the role of Ded1 in the cell. To this end, we used a modified PAR-CLIP technique to identify RNA substrates of Ded1 in vivo [24]. We identified the Small Cytoplasmic RNA 1 (SCR1) as a major noncoding RNA that crosslinked to Ded1. SCR1 is the RNA component of the signal recognition particle (SRP) that is important for the co-translational translocation of polypeptides into the lumen and membrane of the endoplasmic reticulum (ER; reviewed in [25–28]). SRP-dependent translation is conserved across all organisms, from prokaryotes to eukaryotes, including a highly reduced version for chloroplasts [29–31]. It seemed possible that Ded1 was implicated in SRP-dependent translation.

The SRP-dependent translation is a complicated and multi-step process that is still incompletely understood and that involves a number of still-controversial elements. In eukaryotes, the SRP consists of the noncoding RNA (7S or 7SL in metazoans) and six SRP proteins (SRP9, SRP14, SRP19, SRP54, SRP68, and SRP72). The SRP RNA consists of two functional elements called the Alu and S domains [32,33]. The yeast SRP complex consists of the SCR1 RNA and the equivalent proteins, except Sec65 substitutes for the smaller SRP19 and the novel SRP21 protein replaces SRP9 (reviewed in [34]). Moreover, in yeast, SRP14 forms a homodimer on the Alu domain of SCR1, which is in contrast to the heterodimer of SRP14-SRP9 in metazoans [34–36]. The role of the yeast SRP21 protein is unclear, although it is considered the structural homolog of SRP9 [37]. SRP54 and Sec65 interact with the extremity of the S domain of SCR1, and SRP68 and SRP72 interact at the junction between the Alu and S domains [26,34]. Yeast lacks the “classical” structure of the Alu domain that includes helices 3 and 4, and it contains additional hairpins between the Alu and S domains; it is about 75% bigger (Figure 1; [32,33]). The structure and role of these additional hairpins are largely unknown. Eukaryotes lack helix 1, which is found in prokaryotes.

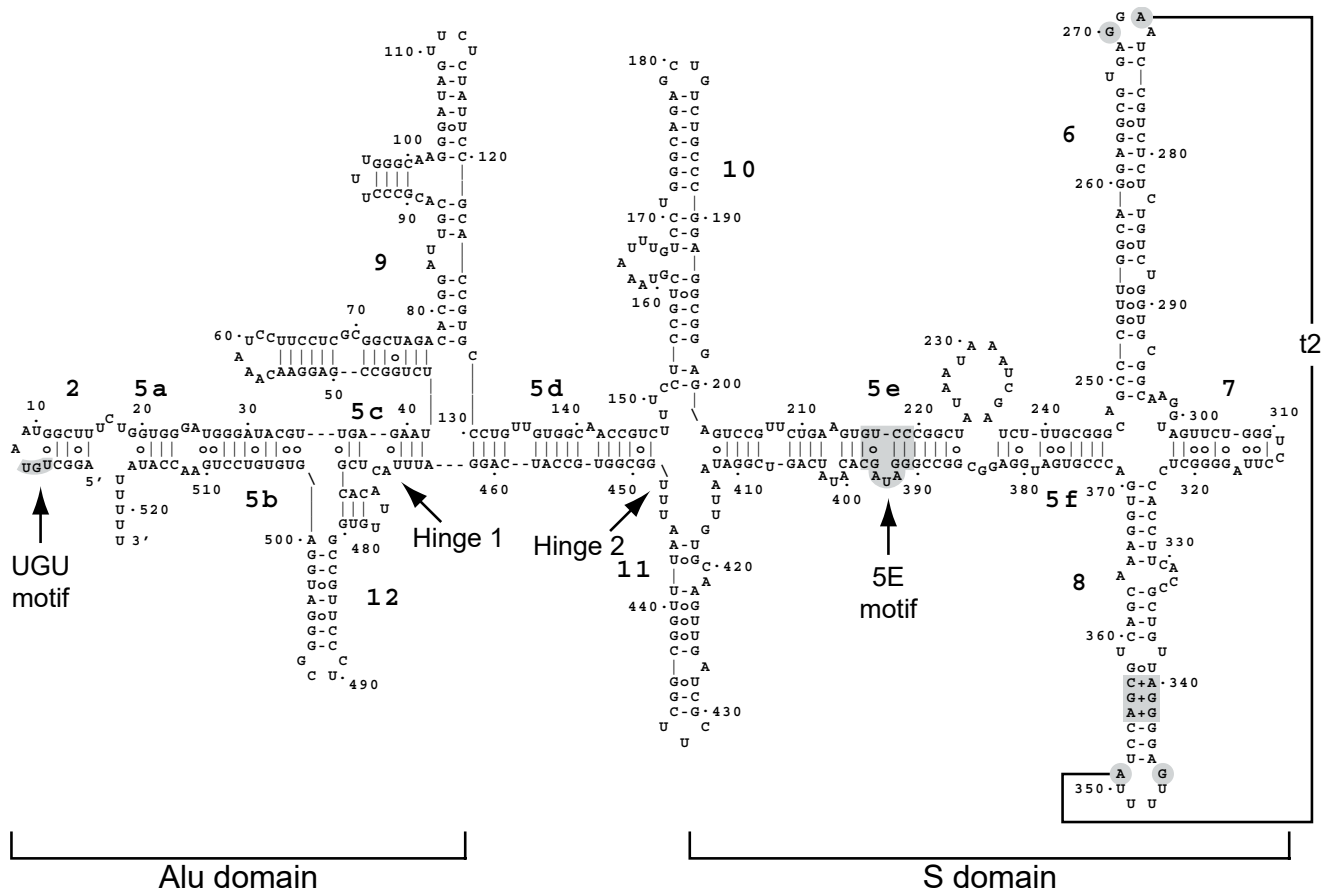


Figure 1. Secondary structure model of yeast SCR1 from Zwieb et al. [32]. The model is based on phylogenetically conserved features found in SRP RNAs and on structural probing experiments [32,33]. Yeast and other fungal SRP RNAs are unusual in that they are much larger than in other organisms, and they lack the characteristic structure consisting of hairpins 3 and 4 of the Alu domain. Yeast has additional hairpins 9, 10, 11, and 12 that are poorly characterized and that have other proposed secondary structures. Conserved sequence motifs and tertiary interactions are shown in gray.

In the classical interpretation, the SRP associates with the ribosome during translation when the SRP54 GTPase binds the hydrophobic signal peptide as it emerges from the exit channel of the 60S ribosomes as a ribosome–nascent chain complex (RNC; reviewed in [25–27]). This causes the ribosomes to pause translation and permits the SRP-ribosome complex to associate with the SRP receptor (SR) on the ER that consists of the membrane-associated SRP101 and the integral membrane protein SRP102 (SR α and SR β , respectively, in metazoans). In yeast and metazoans, SRP14 and the Alu domain of the SRP RNA play an important role in this “pausing” by blocking the GTP-dependent elongation factor eEF2 from binding at the GTPase-associated center near the mRNA entry channel at the interface between the 40S and 60S ribosomes [36,38,39]. The interactions with the ribosomes depend on the SRP proteins; human 7SL RNA does not bind the ribosomes by itself [40]. The SRP-ribosome complex eventually associates with the Sec61 translocon on the ER membrane, the SRP dissociates from the ribosome, and translation continues with the polypeptide inserted into the ER lumen or membrane. Ded1 could be intimately associated with this process.

We find that Ded1 is an SRP-associated factor. Ded1 is genetically linked to the SRP proteins, and it is associated with SRP complexes in pull-down experiments and sucrose gradients *in vivo*. The purified recombinant SRP proteins physically interact with Ded1 *in vitro*. Ded1 is extensively crosslinked to SCR1 RNA in *in vivo* qtPAR-CLIP (quick-time photoactivable ribonucleoside crosslinking-and-immunoprecipitation) experiments. Moreover, fluorescence microscopy shows that Ded1 is associated with mRNAs at the ER

membrane in the cell. RNA-binding assays show that Ded1 has a high affinity for SCR1 RNA. Finally, the ATPase activity of Ded1 is inhibited by SRP21, and it is inhibited much more when SRP21 is associated with SCR1 than with other RNAs. We propose a model where Ded1 plays an important role in the SRP-dependent translation of proteins.

2. Results

2.1. Ded1 Associated with SRP Factors In Vivo

2.1.1. Ded1 Crosslinks to SCR1 RNA

We previously used a modified PAR-CLIP technique, which we call quick-time PAR-CLIP (qtPAR-CLIP), to identify RNA substrates of Ded1 in vivo [24]. In this work, we found that the vast majority of the recovered RNA fragments crosslinked to Ded1 are from mRNAs and ribosomal RNAs, while smaller amounts are from tRNAs and small nuclear RNAs (snRNA). We performed these experiments under normal growth conditions and under brief glucose-depletion conditions, which are known to rapidly attenuate the majority of translation with little effect on the overall mRNA abundance [41–43]. These glucose-depletion results are consistent with Ded1 interacting with actively translated mRNAs because there is a 50% reduction in the percentage of mRNAs recovered, and there is a significant shift to crosslinked mRNAs that encode proteins involved in metabolic shifts. In both growth conditions, the vast majority of the recovered mRNA fragments are on the coding regions, which provided further evidence that the interactions are on actively translating mRNAs [24].

In this work, we did not recover any noncoding RNAs (ncRNA) with the exception of SCR1 and SRG1. SRG1 negatively regulates the transcription of the *SER3* gene as capped and polyadenylated RNAs [44]. We recover fewer *SRG1* RNA fragments under glucose-depletion conditions [24]. In contrast, we recover more crosslink fragments of SCR1 RNA under glucose-depletion conditions. SCR1 RNA is part of the SRP complex involved in translating and transporting polypeptides into the lumen of the ER [25–28]. The four-fold increase in crosslinks under the glucose-depletion conditions is consistent with a role in translation as there should be an increased expression of vacuolar proteins.

In this current work, we made a heat map that shows the location and frequency of the recovered sequences on SCR1 RNA (Supplementary Figure S1). The crosslinks were concentrated on stem 5a–5c and hairpin 12 of the Alu domain and on hairpins 6, 7, and 10 and one side of stem 5e under standard growth conditions (Supplementary Figure S1A). Under glucose-depletion conditions, the distribution was more widespread, although oddly we recovered no fragments corresponding to hairpin 12 and part of stem 5b (Supplementary Figure S1B). These data are consistent with Ded1 interacting extensively with the SCR1 RNA.

2.1.2. Ded1 Associated with SRP Proteins on Sucrose Gradients

These results are consistent with our previous observations that Ded1 cosediments and associates with complexes containing SRP proteins on polysome sucrose gradients, as determined using pull-down experiments and mass spectroscopy analyses [13]. These data showed that Ded1 and SRP proteins SRP14, SRP21, SRP54, and SRP68 sediment at a position corresponding to ~26S (Supplementary Table S1). This is consistent with Ded1 sedimenting in ribonucleoprotein (RNP) complexes of a similar size to those for the SRP proteins.

We subsequently performed pull-down experiments of the sucrose-gradient fractions with Ded1-specific IgG (Supplementary Table S2). We found that SRP14, SRP21, Sec65, and SRP68 were in stable complexes associated with Ded1 on the sucrose gradients that were pulled down with Ded1-specific IgG. These results indicated that Ded1 might be associated with mRNAs encoding ER proteins.

2.1.3. Ded1 Stably Associated with SCR1 RNA and SRP Proteins in Extracts

To elaborate on these observations, we performed pull-down experiments on yeast extracts with IgG against Ded1 and then subjected the recovered material to Northern

blot analysis with a ^{32}P -labeled DNA probe against SCR1. We used a probe against PGK1 mRNA as a positive control because it also was found to crosslink efficiently to Ded1 and a probe against RPL20B mRNA as a negative control as we obtained little crosslinking on this RNA, even though it is a highly expressed mRNA [45]. However, the resulting signals were insufficiently sensitive. This was not unexpected as Ded1 interacts with a large number of mRNAs, and the RNAs of interest represented a small fraction of these total RNAs [14,46]. Hence, we performed RT-PCR on the samples using oligonucleotides specific to the three RNAs. Both SCR1 and PGK1 RNAs were amplified much more in the fractions pulled down with Ded1-specific IgG than in the control fractions that were pulled down with pre-immune IgG (Figure 2A). In contrast, RPL20B mRNA was weakly amplified in both cases. Hence, this was further evidence that Ded1 was associated with SCR1 RNA in vivo.

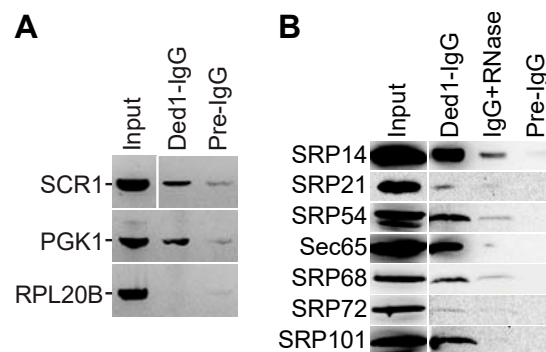


Figure 2. Ded1-IgG pull-downs of yeast extracts. Ded1-specific IgG (Ded1-IgG) or IgG from pre-immune serum (Pre-IgG) were used to recover the associated factors. Input, a fraction of the yeast extract used in the pull-down experiments was directly loaded onto the gel or RT-PCR amplified. (A) Purified RNA from yeast extracts (~20% of input) or from IgG pull-downs was reverse transcribed and PCR amplified for 25 cycles with gene-specific oligonucleotides. The resulting products were electrophoretically separated on a 2% agarose gel containing ethidium bromide, and the products were visualized with a Gel Doc XR+ (Bio-Rad, Hercules, CA, USA). (B) Western blot analysis of HA-tagged SRP proteins. Proteins were electrophoretically separated on a 12% SDS-PAGE, transferred to nitrocellulose membranes, and then revealed with anti-HA IgG. Input, 40 μg (~10%) of the yeast extract was directly loaded on the gel. Ded1-IgG, Ded1-specific IgG was used to pull down Ded1-associated proteins. IgG+RNase, complexes bound to Ded1-IgG-protein A beads were digested with RNase A (1 mg/mL) prior to washing and elution. Note that the same exposure was used for the input, Ded1-IgG, and pre-IgG in panel A, while somewhat shorter exposures were used for the input in panel B.

It was possible that Ded1 interacted with the SCR1 RNA independently of the SRP proteins. To test this, we performed Ded1-IgG pull-down experiments, SDS-PAGE separation, and Western blot analyses of the recovered proteins. However, we were initially only able to obtain antibodies against Sec65 (generously provided by Martin R. Pool; [47]). Hence, we cloned all the SRP genes with amino-terminal HA tags, and we performed Ded1-IgG pull-downs with strains independently expressing each tagged protein (Figure 2B). We recovered a significant amount of SRP14, SRP54, Sec65, and SRP101. Likewise, we digested the Ded1-IgG-bound complexes with RNase A prior to elution to determine if these complexes depended on SCR1 RNA; in all cases, the signals for the SRP proteins were reduced, but the signals were still more than for the pre-immune IgG control (Figure 2B). Oddly, we detected little HA-tagged SRP21 even though it was prominent in our previous mass spectrometry analyses (Supplementary Tables S1 and S2; [13]). Moreover, we detected little HA-SRP21 in yeast extracts even though it is of similar size and has similar expression levels as SRP14 (Figure 2B; Supplementary Table S3). It was possible that the HA tag increased the proteolytic degradation of the protein during extraction or that the HA tag by itself was proteolytically removed. Thus, these results showed that Ded1 interacted with complexes containing the SRP proteins and that these complexes were stabilized via SCR1

RNA (Figure 2B). Notably, the bound complexes also contained the SR receptor SRP101, which binds with SRP complexes associated with the ER during translation [25,34]. We did not detect SRP102 but it contains an integral membrane domain that could limit its recovery. Thus, Ded1 is physically associated with the SRP complex in vivo.

2.2. Ded1 Was Genetically Linked to SRP Proteins

2.2.1. Multicopy Suppression of Ded1 Mutant

We next tested to see if there was a genetic link between Ded1 and the SRP proteins as we previously demonstrated for the nuclear and cytoplasmic cap-associated proteins [13]. We used the same cold-sensitive mutant F162C of Ded1 in the *ded1::HIS3* deletion strain and overexpressed the SRP proteins and SCR1 RNA from the pMW292 and pM299 plasmids [47,48]. Liquid cultures were serially diluted and spotted on 5-fluoroorotic acid (5-FOA) plates that were incubated at 18 °C, 30 °C, and 36 °C (Supplementary Figure S2). The results showed a slight enhancement in growth at 18 °C that was consistent with a genetic interaction between Ded1 and the SRP complex, but the signal was too weak to demonstrate a clear link. The weak multicopy suppression was not unexpected because Ded1 is implicated in the expression of multiple mRNAs that are not associated with SRP complexes [14,46]; the expression of these mRNAs would be insensitive to the overexpressed SRP factors. Thus, it was possible that the SRP complex would be more sensitive to the level of Ded1 expression than vice versa.

2.2.2. Constitutive and Null Expression of Ded1 and SRP Proteins

Previous work has shown that the loss of any SRP component leads to a slow-growth phenotype [49–51], although yeast cells are eventually able to adapt to this loss [52,53]. Thus, we obtained yeast strains with the *DED1*, *SRP14*, *SRP21*, *SEC65*, *SRP68*, *SRP72*, and *SRP101* genes under the control of a tetracycline-regulated promoter that could be suppressed with doxycycline [54]. Unfortunately, SRP54 under the tetracycline promoter was not available. Cultures of the different strains were grown in liquid culture, serially diluted, and spotted on agar plates in the presence or absence of 10 µg/mL of doxycycline. All the strains except *SRP101* showed reduced growth with the constitutive expression of the proteins, which was most apparent at 18 °C (Supplementary Figure S3). Thus, the unregulated overexpression of most of the proteins resulted in reduced viability.

When the expression of all the proteins was shut off in the presence of doxycycline, all the strains showed strongly reduced growth except *SRP21*, *SEC65*, and *SRP101*, which showed a slight reduction. The Western blot analysis of liquid cultures of *TET-SRP21* and *TET-SEC65* grown for up to 24 h in the presence of 10 µg/mL of doxycycline showed no diminution in protein level when probed with SRP21-IgG or Sec65-IgG, respectively. This indicated that either the *TET* promoter was not completely shut down with doxycycline in these strains or that the proteins were particularly stable. Interestingly, *TET-SRP21* actually grew slightly better in the presence of doxycycline, which further indicated that the constitutive expression of the proteins was detrimental (Supplementary Figure S3). The constitutive overexpression of Ded1 was previously shown to inhibit cell growth [55,56].

2.2.3. Ded1 Multicopy Suppression of SRP Protein Depletions

We transformed the different *TET* strains with a plasmid containing *DED1* under the control of the very strong glyceraldehyde 3-phosphate dehydrogenase (*GPD*) promoter and compared it with cells transformed with the empty plasmid and with wildtype yeast cells [57]. We likewise transformed the cells with a plasmid expressing the mutant Ded1-F162C protein that had reduced ATP binding and enzymatic activity [48]. As expected, the yeast strains *TET-SRP21* and *TET-SEC65*, which stably retained the SRP proteins, showed reduced growth on the plates due to the inhibitory effects of the overexpressed Ded1 (Figure 3). In contrast, *SRP14*, *SRP68*, and *SRP72* showed enhanced growth despite the inhibitory effects of Ded1 (Figure 3). The *ded1-F162C* mutant showed little or no stimulatory effect, which indicated that the enzymatic function of Ded1 was important for enhanced

growth. Thus, the high expression of Ded1 partially suppressed the slow-growth phenotype of strains depleted for SRP proteins, and this result established a genetic link between Ded1 and the SRP complex.

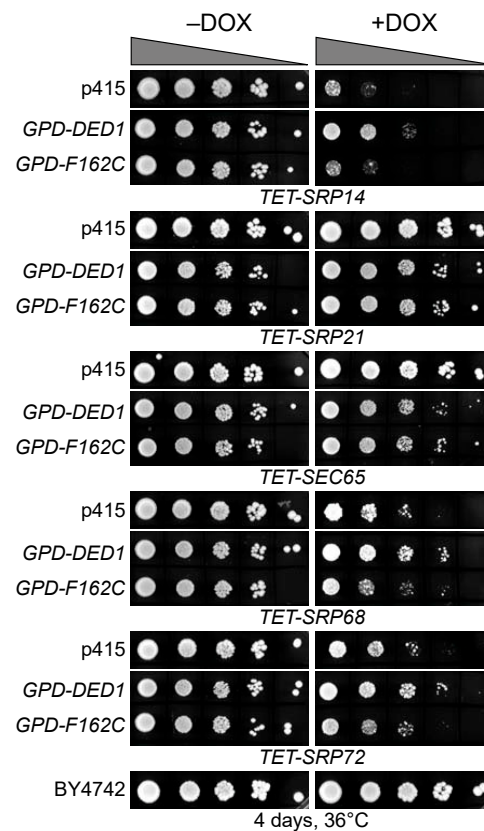


Figure 3. Ded1 multicopy suppression of SRP protein depletions. Cells of the indicated strains with the *TET* promoter were grown in SD-LEU medium, serially diluted by a factor of 10, and spotted on SD-LEU agar plates with (+DOX) or without (–DOX) 10 µg/mL of doxycycline. Cultures were grown for 4 days at 36 °C. p415, empty *LEU* plasmid; *GPD-DED1*, Ded1 in p415 with the high-expression *GPD* promoter and *CYC1* terminator; *GPD-F162C*, a Ded1 mutant with reduced ATP binding and enzymatic activity [48]. BY4742, a wildtype yeast strain showing unimpeded growth. The phenotypes were most apparent at 36 °C, but similar effects were obtained at 30 °C.

2.3. *In Situ* Localization of Ded1 and SRP Proteins

2.3.1. Ded1 Was in Cellular Foci Associated with the Endoplasmic Reticulum

The next question we asked was whether Ded1 co-localized with the ER as would be expected if it was associated with SRP-ribosome complexes that were translating mRNAs encoding polypeptides translocated into the ER. However, we and others have shown that Ded1 has a diffuse location within the cytoplasm under normal growth conditions [13,55,58]. Nevertheless, some of the Ded1 protein is sequestered with translation-inactive mRNAs in cellular foci when the translation conditions are altered [55,59]. We reasoned that if polypeptide imported into the ER was transiently blocked then Ded1 would form foci associated with the ER. We used temperature-sensitive (ts) mutants of the Sec61 and Sec62 proteins that form the translocon pore in the ER for the import of SRP-dependent polypeptides during translation [60,61]. At the non-permissive temperature, these mutants block or disrupt the Sec61 channel and ER-associated translation is terminated. As a marker, we used the integrated red-fluorescent-tagged amino-terminal domain of Kar2 fused to the HDEL ER retention signal (YIPlac204TKC-DsRed-Express2-HDEL; Addgene, Watertown, MA, USA) in the two *sec* strains; Kar2 is an ATPase that functions as a protein chaperone for refolding proteins within the lumen of the ER ([62] and reference therein), and consequently, the Kar2 chimera serves as a marker of the ER lumen. We also used an ATPase-inactive

Ded1-E307Q mutant (Ded1-DQAD) that has a high propensity to form cellular foci with sequestered mRNAs that are no longer undergoing translation.

We first looked at the distribution of proteins under permissive conditions (Figure 4A). The distribution of Kar2-RFP around the nuclear envelope (central cisternal ER) as interconnected tubules (tubular ER) and as a cortical halo inside the plasma membrane of the cell wall (PM-associated ER) was consistent with the locations of the ER in yeast; actively translating ribosomes are associated with all these ERs [63]. Ded1-DQAD-GFP was uniformly distributed in the cytoplasm, largely excluded from the nucleus, and it formed occasional foci that were distributed at various positions in the cytoplasm (Figure 4A). Both the *sec61-ts* and *sec62-ts* strains showed equivalent phenotypes. The intensity of the fluorescence signals of both Kar2-RFP and Ded1-DQAD-GFP was highly variable between cells, which probably reflected different levels of protein expression between cells.

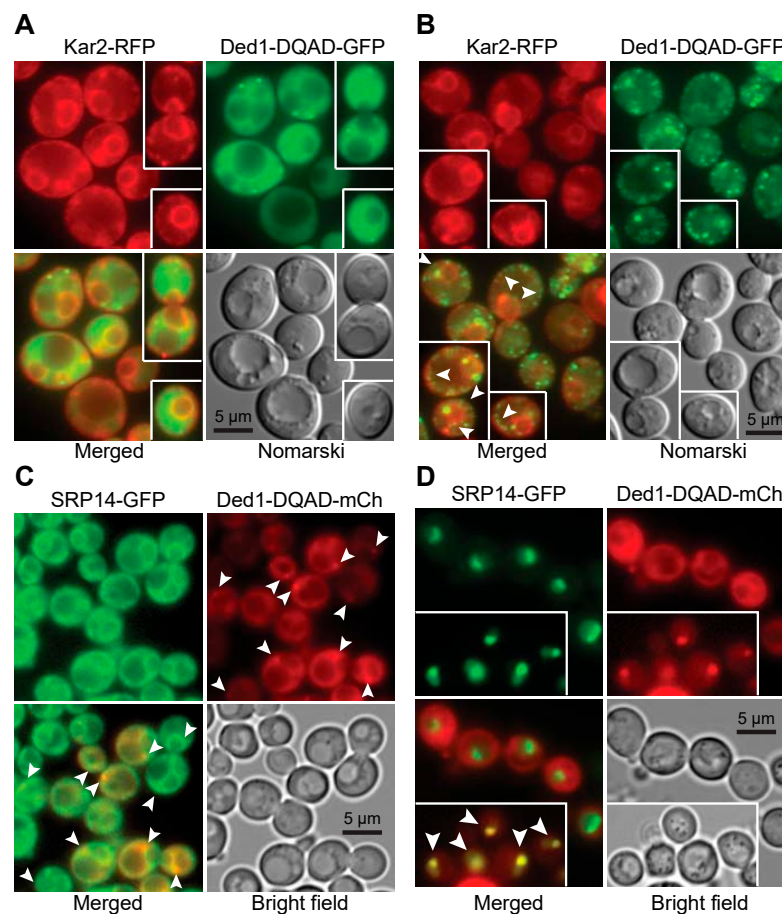


Figure 4. Cellular location of Ded1 relative to the ER and SRP proteins. (A) Ded1-DQAD-GFP was expressed in the *sec62* temperature-sensitive mutant with the integrated *KAR2-RFP* plasmid and grown to an OD600 of 1.0 at 24 °C. (B) The same cells as in A were incubated for 15 min at the non-permissive temperature of 37 °C prior to visualization. The arrowheads indicate positions where chains of Ded1-DQAD-GFP foci co-associated with Kar2-RFP in panels B and C. (C) SRP14-GFP expressed from the chromosome and Ded1-DQAD-mCh expressed off the p415 plasmid were grown to an OD600 of 0.95 at 30 °C. (D) SRP14-GFP was overexpressed off the p413-PL plasmid and Ded1-DQAD-mCh was overexpressed off the p416-PL plasmid until an OD600 of 0.4 at 30 °C in the *xpoI-T539C* yeast strain. Cells in the insert were treated with 10 µg/µL (~200 nM) of leptomycin b for 1 h. The arrowheads indicate the positions where Ded1-DQAD and SRP14 colocalize within a crescent-shaped region of the nucleus.

At 37 °C, Kar2-RFP showed a similar cellular distribution as at 24 °C for both *sec61-ts* and *sec62-ts* mutants, although it showed an increased frequency of aggregates with the ER

(Figure 4B). In contrast, Ded1-DQAD-GFP showed a pronounced increase in the number of foci that were highly variable in size (Figure 4B). Many of these foci were closely associated with Kar2-RFP, particularly as a chain of foci on the cytoplasmic side of the ER around the plasma membrane, where the PM-associated ER was expected to be located, and as a chain of foci corresponding to tubular ER (arrowheads, Figure 4B). Both the *sec62-ts* and *sec61-ts* strains showed similar phenotypes. In some cases, the Kar2-RFP aggregates and Ded1-DQAD-GFP foci were near each other. Thus, Ded1 was associated with mRNAs that were no longer undergoing translation in close proximity to the ER at the non-permissive temperature. This result was consistent with previous work that showed that Ded1 is recovered with membrane-associated ribosomal–protein complexes [64].

We next asked if the SRP proteins showed similar properties. We used GFP-tagged SRP14 and SRP21 proteins that were expressed off the chromosome (GFP bank, Thermo Fisher Scientific, Waltham, MA, USA) and the plasmid-encoded Ded1-DQAD-mCh mutant. The SRP14-GFP showed a weak but uniform signal in all the cells where the protein was concentrated on the ER (Figure 4C). SRP21-GFP showed a similar profile. In contrast, the plasmid-expressed Ded1-DQAD-mCh showed highly variable expression. We used cells grown under wildtype conditions or depleted for glucose, which promoted the formation of cellular foci. However, depending on the cellular growth, we obtained a significant number of foci associated with the ER even under wildtype growth (arrowheads, Figure 4C). Thus, Ded1 was in close proximity to both the ER and the SRP proteins in the cell.

2.3.2. Overexpressed SRP Proteins Accumulated in the Nucleus and Nucleolus

The biogenesis and metabolic pathway of the SRP RNP is complex, and it involves a large number of different steps (reviewed in [31,65,66]). In yeast, the SRP proteins SRP14, SRP21, SRP68, and SRP72 are assembled on the SCR1 RNA probably in the nucleolus. Sec65 is in the nucleus but there is some ambiguity about whether it accumulates in the nucleolus as well, although the equivalent mammalian SRP19 protein is found there [31,67,68]. The partially assembled SRP complex is then exported to the cytoplasm through the XpoI/CrmI nuclear pore complex whereupon it binds with SRP54, which subsequently associates with the signal sequence of the partially translated polypeptide and causes the SRP to assemble on the 80S ribosomes. We previously showed that Ded1 actively shuttles between the nucleus and cytoplasm using the XpoI and Mex67 nuclear pores [13]. Thus, it was possible that Ded1 was associated very early with the SRP complex within the nucleus, and that it was important for the biogenesis of the SRP or associated with the export of the complex.

The XpoI nuclear pore is known to export multiple cargoes, including ribosomal subunits, certain small nuclear RNAs, some viral RNAs, and the assembled SRP complex [67–70]. We used a yeast strain with a mutant *xpoI* allele that is sensitive to the bacterial toxin leptomycin b from *Streptomyces* to test whether Ded1 was associated with the XpoI-dependent export of the SRP [71]; this strain contains a single mutation (XpoI-T539C) that makes the yeast protein sensitive to the drug [72]. We previously showed that both the Mex67 and XpoI nuclear pore complexes must be disrupted to see a significant accumulation of Ded1 in the nucleus [13]. We transformed this strain with plasmids expressing Ded1-mCh and with plasmids expressing either SRP14-GFP or SRP21-GFP, and we determined the locations of the tagged proteins.

The plasmid-encoded SRP14-GFP had highly variable expression between cells, but it showed a strong nuclear location that was often concentrated in crescent-shaped regions even in the absence of leptomycin b (Figures 4D and 5A,B). In contrast, SRP21-GFP showed a diffuse location throughout the nucleus, which indicated that the overexpressed protein was not able to assemble or accumulate in the nucleolus (Figure 5C,D). However, it occasionally formed nuclear foci (arrowheads, insert of Figure 5C). The expression of the plasmid-encoded Ded1-DQAD-mCh was likewise highly variable, and it was largely excluded from the nucleus even in the presence of leptomycin b (Figures 4D and 5). However, in some instances with leptomycin b, where Ded1-DQAD-mCh was lightly expressed, we found that the protein accumulated in crescent-shaped regions with SRP14-GFP (arrowheads, insert of

Figure 4D). The Ded1-DQAD mutant binds RNA with a high affinity in the presence of ATP but it cannot hydrolyze the ATP to recycle the complex. Thus, Ded1 could co-localize with the SRP complex in the nucleolus but only under conditions where Ded1 export was blocked. The absence of Ded1-DQAD in the nucleus and crescents in the absence of leptomycin suggested that Ded1 was not needed for SRP assembly and export, but the data could not rule out this possibility.

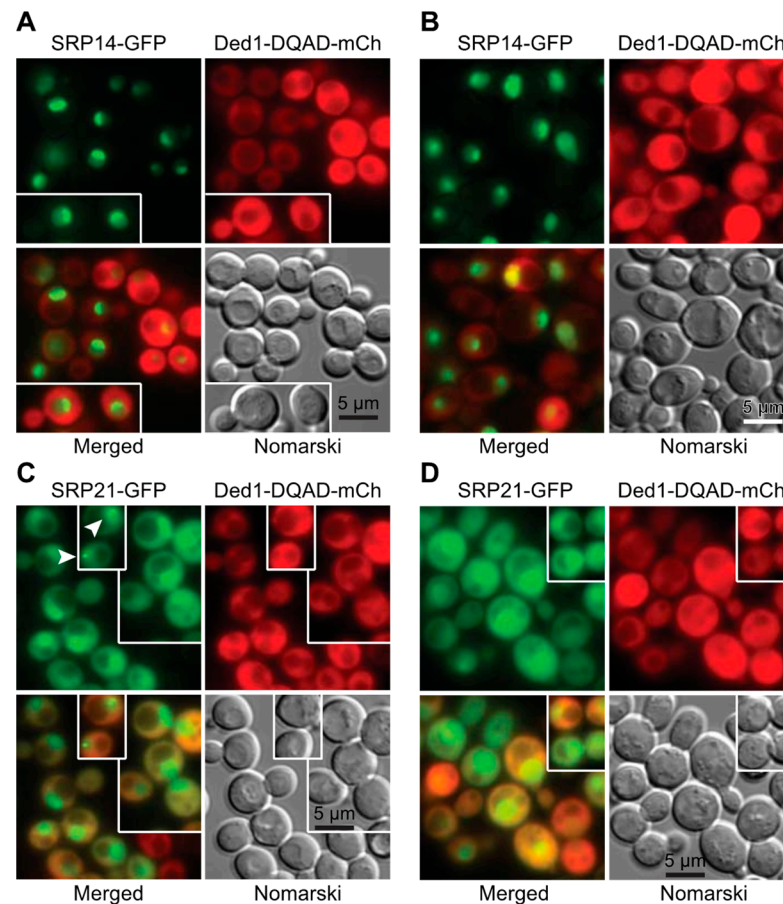


Figure 5. Overexpressed SRP14 and SRP21 accumulate in the nucleus. (A) SRP14-GFP was expressed off the p413 plasmid and Ded1-DQAD-mCh was expressed off the p416 plasmid in the *xpo1-T539C* yeast strain [72] and grown to an OD600 of 0.45 at 30 °C. (B) The same as in A except that the cells were incubated for 60 min in the presence of 10 µg/mL of leptomycin b. (C) Same as A but with cells expressing SRP21-GFP. The arrowheads indicate positions where SRP21 form nuclear foci. (D) Same as C but with cells incubated for 60 min with leptomycin b.

2.4. Ded1 Physically Interacted with SRP Factors

Our data indicated that Ded1 could bind SCR1, associate with the SRP complex, and co-localize with the ER. Moreover, we obtained a genetic link between Ded1 and SRP proteins. However, it was unclear whether Ded1 physically interacted with the SRP proteins or indirectly through the SCR1 RNA (Figure 1). The metazoan SRP14 and SRP9 are known to bind 7SL in the Alu domain, SRP54 and SRP19 bind helices 6 and 8, and SRP68 and SRP72 bind around the junction between helices 5e, 5f, 6, 7, and 8 [26,34]. However, yeast SRP14 is thought to bind the Alu domain as a homodimer and the role of SRP21 to date is largely speculative, although it is considered a structural homolog of SRP9 [35,37]. Yeast Sec65 serves a similar role as SRP19, but it is considerably larger [49,51,73]. The SRP bound on the 80S ribosomes shows an extended structure where the S domain interacts with the exit channel containing the signal peptide and the Alu domain interacts with the entry region of the mRNA [36,38,39]. However, SCR1 contains two hinge regions (Figure 1); it was possible that the SCR1 RNA was folded upon itself in its free form and that this

brought the different regions of the SRP in close proximity. Thus, Ded1 might interact with multiple different SRP proteins.

To test this, we subcloned the genes encoding the different proteins into pET22 and pET19 plasmids and then purified the recombinant proteins expressed in *Escherichia coli* on nickel-agarose columns (Supplementary Figure S4). We then incubated the purified individual proteins or combination therein with purified Ded1, recovered the complexes with Ded1-IgG-Protein-A-Sepharose beads, and separated the recovered proteins via SDS-PAGE (Figure 6).

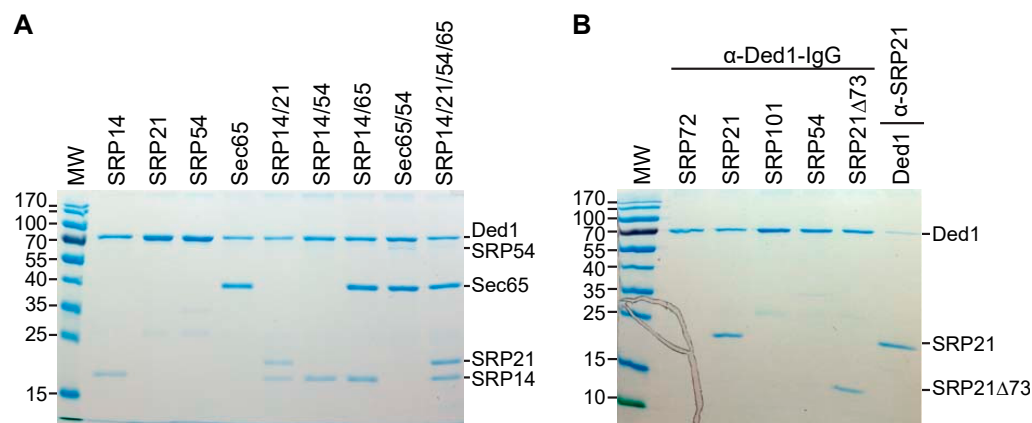


Figure 6. Ded1 physically interacted with the SRP proteins in the absence of RNA. (A) A total of 4 µg of Ded1 was incubated with 4 µg of each SRP protein. The material was incubated for 45 min at 30 °C, immunoprecipitated with protein-A-Sepharose beads with Ded1-specific IgG, separated on a 12% SDS PAGE, and visualized with Coomassie blue. SRP68 and SRP72 migrated close to Ded1 and were consequently not unambiguously separated. (B) The same as A except 6 µg of the SRP proteins was used with 4 µg of Ded1. Proteins were recovered with Ded1- or SRP21-specific IgG as indicated.

The results showed that Ded1 formed stable interactions with SRP14 and Sec65. Unfortunately, SRP68, SRP72, and SRP101 migrated at positions on the SDS-PAGE that overlapped with Ded1; hence, we were not able to obtain unambiguous results but they appeared to have little or no affinity for Ded1. SRP54 did not stably associate with Ded1 by itself. In contrast, SRP21 was not consistently recovered with Ded1, which indicated that it formed weak interactions with the protein (Figure 6). However, SRP21 was consistently recovered with Ded1 in the presence of SRP14, which was consistent with SRP14 and SRP21 forming a stable heterocomplex as previously proposed [37]. Likewise, SRP54 was recovered with Ded1 in the presence of Sec65; this was consistent with the two proteins being in close proximity on the S domain of SCR1 [49,51,73]. Moreover, all four SRP proteins were recovered with Ded1 when incubated together.

The weak interactions between SRP21 and Ded1 were primarily through the amino-terminal domain because deleting the 73 carboxyl-terminal amino acids (SRP21Δ73) did not eliminate this affinity (Figure 6B). Finally, we recovered Ded1 in pull-down experiments with SRP21-specific IgG (Figure 6B). Thus, Ded1 was capable of forming protein–protein interactions with the SRP proteins in the absence of SCR1 RNA. Nevertheless, the presence of SCR1 RNA enhanced the recovery of all the proteins (see Section 2.1).

2.5. The Enzymatic Activity of Ded1 Is Affected by the SRP Proteins

2.5.1. The SRP Proteins Inhibited the ATPase Activity of Ded1

Ded1 is an RNA-dependent ATPase. We previously showed that the nuclear and cytoplasmic cap-associated factors would stimulate the ATPase activity of Ded1 in the presence of RNA [13]. We wondered whether the SRP proteins would alter the enzymatic activity of Ded1 as well and whether it would be preferential for the SCR1 RNA, which would be the authentic substrate for the assembly of the SRP proteins. We tested this with an *in vitro*, T7-polymerase-transcribed SCR1 RNA that was equivalent to the endogenous

SCR1 except that the 5' terminal nucleotide was replaced with a guanosine to facilitate transcription. As a control, we used a fragment of the actin pre-mRNA precursor containing short exon sequences and the entire intron. In addition, the actin transcript was of similar size to SCR1 (605 nts and 552 nts, respectively).

Many of the SRP proteins at nearly a 30-fold excess over Ded1 inhibited the RNA-dependent ATPase activity of Ded1 somewhat for both actin and SCR1, although SRP54 seemed to enhance the activity slightly, especially with actin (Figure 7A). This was not unexpected because the SRP proteins were largely basic and positively charged under the reaction conditions (pH 7.5; Supplementary Table S3); the proteins would be expected to nonspecifically associate with the RNAs and thereby reduce the effective concentration of the RNAs accessible to Ded1. SRP21 showed a much stronger inhibition, especially with SCR1, but it was the most basic (pKi = 11.14) of the SRP proteins. To further elucidate the nature of the inhibition, we compared the ATPase activity of Ded1 with SCR1 and actin RNAs with SRP21. SRP21 is considered the structural homolog of SRP9, and in yeast, it probably forms a complex with a homodimer of SRP14 that binds the Alu domain of SCR1 [35,37]. Thus, we tested to see if SRP14 would enhance the inhibitory effects of SRP21.

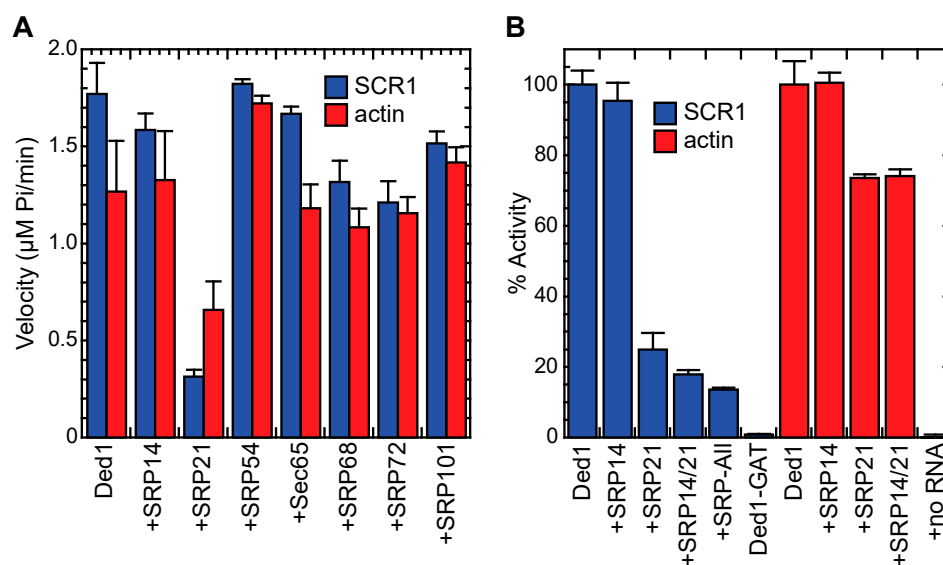


Figure 7. The SRP proteins inhibited the ATPase activity of Ded1. (A) Reactions were undertaken with 7 nM of Ded1, 200 nM of the SRP proteins, 1 mM of ATP, and 23 nM of SCR1 or actin RNA. The reaction velocities were measured over 40 min at 30 °C. (B) Reactions were conducted as in A but with 23 nM of the SRP proteins except for SRP14, which was used at 46 nM to form the homodimer, and 23 nM of RNAs. The reaction velocities were normalized relative to the activity of Ded1 in the presence of the RNA (SCR1 or actin) alone. +SRP-All, Ded1 was incubated with SRP14, SRP21, SRP54, Sec65, SRP68, and SRP72; Ded1-GAT, a Ded1 phosphate-binding (P-loop) mutant that lacks ATPase activity; +no RNA, Ded1 was incubated in the absence of an RNA substrate with the SRP proteins. The means and standard deviations are shown for two independent experiments in panel (A) and for three in panel (B). The lower error bars were deleted for clarity.

Equimolar concentrations of both the actin precursor and SCR1 stimulated the ATPase activity of Ded1, but the stimulation was not equivalent. Moreover, there was variability in the stimulatory effects with different RNA preparations, which probably reflected variability in the folding of the RNAs during preparation. Indeed, others have shown that the smaller human 7SL RNA is difficult to recover as a homogeneous structure in vitro [40]. Thus, to facilitate comparisons, we normalized the activity relative to that of Ded1 with the RNA alone and used the same RNA preparations for comparisons. In addition, we used 8.5-fold less of the SRP proteins to emphasize the differences.

SRP14 may have slightly inhibited Ded1 with SCR1 but it had little effect with actin (Figure 7B). In contrast, SRP21 inhibited the ATPase activity of Ded1 with SCR1 by about

75% but only by 25% with actin. This indicated that there was some nonspecific inhibition but that the strongest inhibition was obtained with the authentic substrate of SRP21. The addition of SRP14 reduced the activity of Ded1 in the presence of SRP21 by an additional 8% for SCR1 but showed no additional reduction with actin. Thus, SRP14 enhanced the SRP21-dependent inhibition of Ded1 with SCR1 RNA. The addition of the other SRP proteins to SCR1 further reduced the activity by about 4%. None of the purified SRP proteins showed any intrinsic ATPase activity in the absence of Ded1, and none of the SRP proteins affected the ATPase activity of Ded1 in the absence of RNA (Figure 7B).

2.5.2. SRP21 Inhibited the SCR1-Dependent ATPase Activity of Ded1

The data indicated that SRP21 in the presence of its authentic substrate was the most effective at inhibiting Ded1. Thus, it was likely that SRP21 bound to the Alu domain of SCR1 formed the most effective inhibitory structure. We tested this with deletions of the S domain (SCR1 Δ S1) and Alu domain (SCR1 Δ Alu; Supplementary Figure S5). Previous work has shown that the folding of mammalian 7SL RNA is difficult, and it needs a temperature step for refolding involving slow cooling in the presence of monovalent cations; moreover, the assembly of the SRP proteins is complicated [40]. The yeast SCR1 RNA is about two-fold larger with a number of additional hairpins, so we anticipated difficulties in obtaining a functional homogenous structure (Figure 1 and Supplementary Figure S5). Thus, we assayed various permutations of pre-incubating the RNA with the various proteins prior to adding the ATP but they all yielded similar results. Ded1 was significantly less active with both SCR1 Δ S1 and SCR1 Δ Alu than full-length SCR1 at equimolar concentrations of RNA but the RNAs were 77% and 58%, respectively, of the size of SCR1. This may account for the reduced ATPase activity, but it was possible that Ded1 was activated by specific structures within the SCR1 RNA that were absent or misfolded in the deletions. SRP21 inhibited the ATPase activity for SCR1 and to a lesser extent actin but it had little inhibitory effect with the SCR1 deletions, which was consistent with a structure-dependent inhibition. We also tested a carboxyl-terminal deletion of SRP21 (SRP21 Δ 73) that lacked the amino acids that did not correspond to those of mammalian SRP9 [37]; it showed significantly less inhibition, which was consistent with it playing a role in the SRP21 interactions with SCR1 and Ded1 (Figure 8A).

The ATPase activity of Ded1 is stimulated by various RNAs containing single-stranded regions but it is most activated by poly(A)-containing RNAs [74]. We repeated the ATPase assays with purified yeast RNA. We needed to use 0.12–0.14 $\mu\text{g}/\mu\text{L}$ of yeast RNA to obtain similar levels of activation of Ded1 as 23 nM of SCR1 (0.0039 $\mu\text{g}/\mu\text{L}$) or actin (0.0044 $\mu\text{g}/\mu\text{L}$; Figure 8B). Thus, yeast RNA was ~30-fold less effective at stimulating the activity. SRP21 and SRP14 showed no inhibitory effects, and they may have actually stimulated the ATPase activity of Ded1 somewhat, perhaps by acting as RNA chaperones to increase the accessibility of the RNA to Ded1. However, the yeast RNA was a heterogenous mix that may have had both activating and inhibitory RNAs. Thus, we repeated these experiments with yeast tRNAs and poly(A) RNA at 0.12 $\mu\text{g}/\mu\text{L}$ (Figure 8C). Both RNAs needed ~30-fold higher concentration than for SCR1 to stimulate the ATPase activity of Ded1 to similar levels but SRP21 had little effect on the activities. Thus, Ded1 and SRP21 preferentially bind RNAs with certain sequences or structural features.

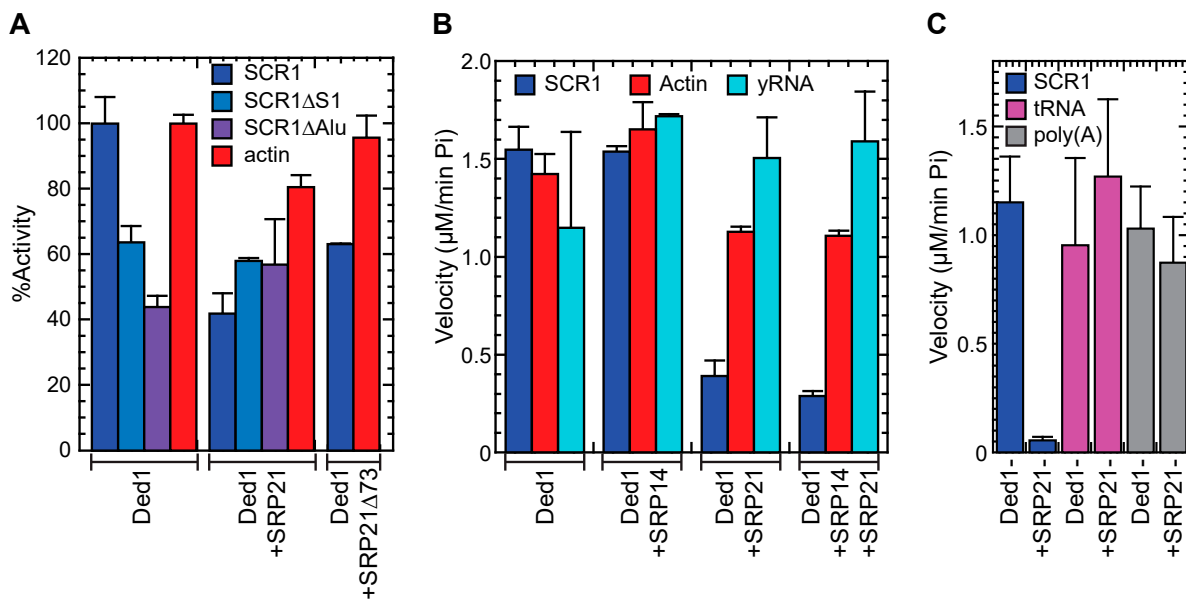


Figure 8. The RNA-dependent effects of SRP21 on the ATPase activity of Ded1. (A) Ded1 was pre-incubated with the RNAs at 30 °C for 30 min. SRP21 or SRP21Δ73 was then added at 200 nM with 1 mM of ATP, and the ATPase velocity was measured over 40 min. The means and standard deviations are shown for two independent experiments. (B) Ded1 at 7 nM was incubated with 23 nM of SCR1, 23 nM of actin, or 0.14 μg/μL of yeast RNA and with 1 mM of ATP. SRP21 was used at 23 nM and SRP14 at 46 nM (to form a homodimer). The reaction velocities were measured over 40 min at 30 °C. The means and standard deviations are shown for three independent measurements for SCR1 and actin and for two independent measurements for yeast RNA. (C) Reactions were performed as in B. Ded1 at 7 nM was incubated with 23 nM of SCR1 (equivalent to 0.0039 μg/μL) or with 0.12 μg/μL of tRNA or poly(A). SRP21 was used at 200 nM. The means and standard deviations are shown for three independent measurements. The lower error bars were deleted for clarity.

2.6. The RNA Binding Properties of Ded1 and SRP21

2.6.1. Ded1 Bound Actin and SCR1 RNAs with High Affinity, but SRP21 Preferred SCR1

The previous results indicated that Ded1 was either blocked from binding the SCR1 RNA or that its ATPase activity was inhibited by protein–protein contacts with SRP21 bound on the RNA. To test this, we conducted electrophoretic mobility shift assays (EMSA) with the different proteins and RNAs. Our previous work showed the strong, concentration-dependent binding of Ded1 to short oligonucleotides in the presence of AMP-PNP with a $K_{1/2}$ of ~40 nM and weak binding in the presence of ADP or in the absence of a nucleotide [75]. We repeated these experiments with the longer RNAs, but we separated the products on agarose gels containing ethidium bromide. Similar results were obtained when the gels were run in the absence of ethidium bromide, which was then soaked into the gels after electrophoresis.

A 5- to 10-fold excess of Ded1 was able to displace the majority of both SCR1 and actin (Figure 9A). SCR1 typically migrated as a distinct band but actin often showed more heterogeneity, which probably reflected more profound conformational heterogeneity. This varied somewhat between RNA preparations. In contrast, SRP21 preferentially bound SCR1 RNA over actin (Figure 9B). Moreover, it seemed to form large molecular-weight aggregates that only partially migrated into the gels. Deleting the carboxyl-terminal sequences of SRP21 (SRP21Δ73) largely eliminated the binding affinity, indicating that these sequences were either important for binding or for maintaining the correct conformation of the protein (Figure 9C).

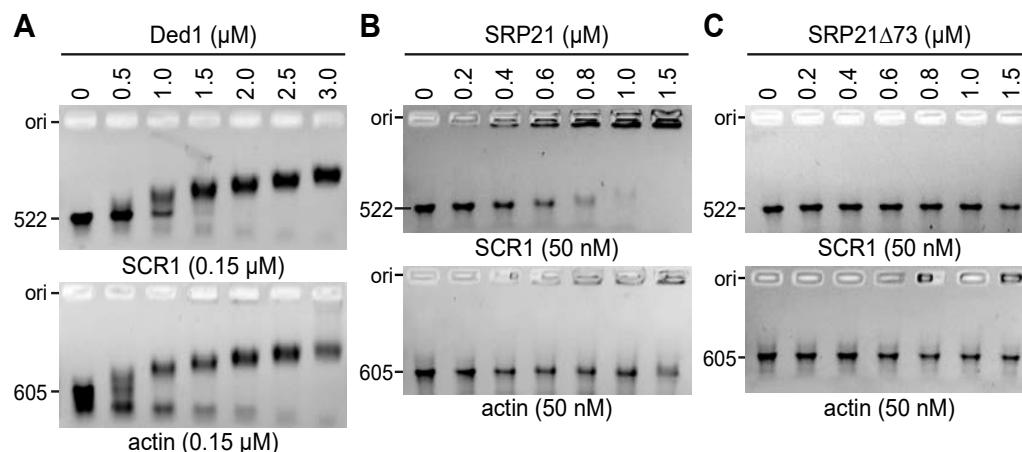


Figure 9. RNA-binding assays of Ded1 and SRP21. (A) Ded1 binds SCR1 and actin with similar affinities. The indicated quantities of the Ded1 protein were incubated with 0.15 μM of the indicated RNAs and then separated on a 1% agarose gel in the presence of ethidium bromide. Ori, loading well of agarose gel. (B) The indicated quantities of the SRP21 proteins were incubated with 50 nM of the indicated RNAs and separated on a 1% agarose gel. (C) SRP21 was deleted for the 73 carboxyl-terminal residues that are not structurally conserved in mammalian SRP9.

2.6.2. Ded1 and SRP21 Bound SCR1 and Actin RNAs Separately

We next asked what effect SRP21 would have on Ded1 binding. The results showed that SRP21 had little effect on Ded1 binding for both SCR1 and actin RNAs, but the retarded bands tended to migrate as higher molecular-weight complexes in the presence of SRP21 that were retained in the wells of the gel (Supplementary Figure S6A). We previously showed that the carboxyl-terminal domains of DEAD-box proteins, including Ded1, are important for high-affinity binding to RNAs [56]. Consistent with this, deleting 78 amino acids from the carboxyl terminus of Ded1 largely eliminated RNA binding (Supplementary Figure S6B). However, the addition of SRP21 had little effect on Ded1ΔC binding (Supplementary Figure S6C).

3. Discussion

Our experiments show that Ded1 is an SRP-associated factor. It physically interacts with the SCR1 RNA and many of the SRP proteins both *in vitro* and *in vivo*. It is genetically linked to these proteins, and it cosediments with the SRP factors in sucrose gradients. The RNA-dependent ATPase activity of Ded1 is inhibited by SRP21 and this inhibition is much more pronounced in the presence of SCR1 RNA, the authentic substrate of SRP21. Although there is probably conformational heterogeneity of the *in vitro*-generated RNAs, SRP21 preferentially binds SCR1 RNA over actin RNA, which indicates that it contains or forms the necessary elements for high-affinity SRP21 binding. Likewise, the ATPase activity of Ded1 is preferentially activated by SCR1 and actin RNAs over an equivalent concentration of whole yeast RNA, tRNA, or poly(A) RNA, which indicates that it recognizes specific features or structures of these RNAs. The nature of these features or structures is unclear. Finally, Ded1 co-localizes in cellular foci with the ER-associated mRNAs, and it occasionally co-localizes with SRP proteins in the nucleolus.

The role of SRP21 to date is largely unclear. It is considered the structural homolog of metazoan SRP9, which forms a heterodimer with SRP14 on the Alu domains of 7SL RNA, even though there is little or no sequence homology [37]. The amino-terminal residues of SRP21 are capable of forming similar structural features as SRP9, but it is over 80% bigger; the carboxyl-terminal sequences are thought to compensate for the abbreviated Alu domain of yeast SCR1, which lacks the characteristic hairpins H3 and H4 [37]. Moreover, yeast SCR1 is about 75% bigger than metazoan 7SL, and it contains additional structures between the Alu and S domains [32,33]. SRP21 may be needed to stabilize or form the correct

conformation of the SCR1 RNA and, thus, it may need to recognize multiple structures or features of the RNA. In contrast, it has a weak affinity for the actin RNA. The carboxyl-terminal sequences of SRP21 are important for this affinity. This is consistent with SRP21 forming a complex with the SRP14 homodimer as previously proposed [37].

SRP21 inhibits the RNA-dependent ATPase activity of Ded1 but it is much more effective in the presence of SCR1 RNA than actin RNA. In contrast, Ded1 binds SCR1 and actin RNAs with similar affinities and it is activated to similar extents. Under these circumstances, one would expect SRP21 to reduce Ded1 binding to SCR1 but not to actin because SRP21 would reduce the number of potential binding sites for Ded1 on SCR1. But this is not the case, and if anything, SRP21 seems to enhance Ded1 binding to SCR1 slightly. The enzymatic inhibition is due to protein–protein contacts but SRP21 is less stably associated with Ded1 in the absence of SRP14 or SCR1 RNA. Thus, SRP21 probably forms a specific inhibitory structure with Ded1 in the presence of SCR1 RNA. This is consistent with the functional regulation of the ATPase activity of Ded1 in the context of the SRP complex.

Ded1 is an ATP-dependent RNA-binding protein, and it is capable of forming long-lived complexes with RNA in the presence of a nonhydrolyzable analog of ATP *in vitro* [8]. Ded1 is considered a translation-initiation factor ([14,15] and references therein) but crosslinking studies on DDX3 show most of the interactions on the open reading frames of a subset of the mRNAs [76]. We obtained similar results with Ded1 [24]. Thus, Ded1 remains associated with the ribosomes during translation elongation, which can be seen in polysome profiles as well [13]. Ded1 likewise is found with membrane-associated ribosomes [64]. Thus, Ded1 may play important roles in translation elongation as well as in initiation, including membrane-associated translation.

Ded1 is associated with 90S ribosomal precursors, which may indicate a role of Ded1 in SRP assembly in the nucleolus [77]. We do see the occasional co-localization of the Ded1-DQAD mutant with overexpressed SRP14 in crescent-shaped structures in the nucleus that are consistent with this possibility but SRP21 has a diffuse location within the nucleus and it is never seen concentrated in the crescent-shaped structures. Thus, it may associate with the SRP complex outside the nucleolus or it may be transiently located within the nucleolus, as has been proposed for Sec65 [67]. Thus, we cannot rule out a role for Ded1 in the biogenesis of the SRP complex in the nucleus that is regulated by SRP21. Under these circumstances, Ded1 may associate early with the SRP complex and remain attached even when the complex binds the 80S ribosomes. This would provide a possible mechanism by which ER-specific mRNAs are selected for translocation on the ER. Interestingly, DDX3 crosslinks to 7SL RNA as well [76]. Thus, although metazoans lack a clear equivalent to SRP21, DDX3 may also be intimately connected to SRP-dependent translation.

On the basis of these observations, we propose the following model for the role of Ded1 (and DDX3-like proteins) in membrane-associated translation. Ded1 interacts with cap-associated factors and with Pab2 bound on the 3′ poly(A) tail of the mRNA. The 3′ UTR is considered important for the SRP-dependent targeting of mRNAs (reviewed in [78]), but the SRP is not known to directly interact with the mRNA and it may interact through another RNA-binding protein [79]. Ded1 (and DDX3) could serve this role as it interacts with both 5′ and 3′ components of the mRNA ([13,16] and references therein). Ded1 remains attached to the mRNA during scanning by the 48S PIC, the formation of the 48S IC at the AUG start codon, and the eventual assembly of the 80S ribosomes (Figure 10A). This is consistent with crosslinking experiments of ribosomal RNA that show Ded1 near the mRNA entry channel [24,46]. The RNA-dependent ATPase activity of Ded1 is uninhibited and it is able to translocate on the mRNA with the ribosomes through rapid cycling between the “open” and “closed” conformations, and it may further stabilize the ribosome-mRNA complex during scanning, assembly, and translation [14]. During this time, an inactive form of the SRP may associate with the mRNA-ribosome-Ded1 complex through postulated 3′ UTR factors that are specific for SRP-dependent translation while the ribosomes are still part of the soluble fraction during a pioneering round of translation, as previously proposed [79]. The Alu domain of the SRP would be easily displaced from the ribosomes via elongation

factors [80]. Ded1 may play an important role in the assembly and stabilization of this complex because it can interact with all the relevant factors. Alternatively, Ded1 may help associate the SRP on the ribosomes once the signal peptide is sufficiently long according to the classical model [81].

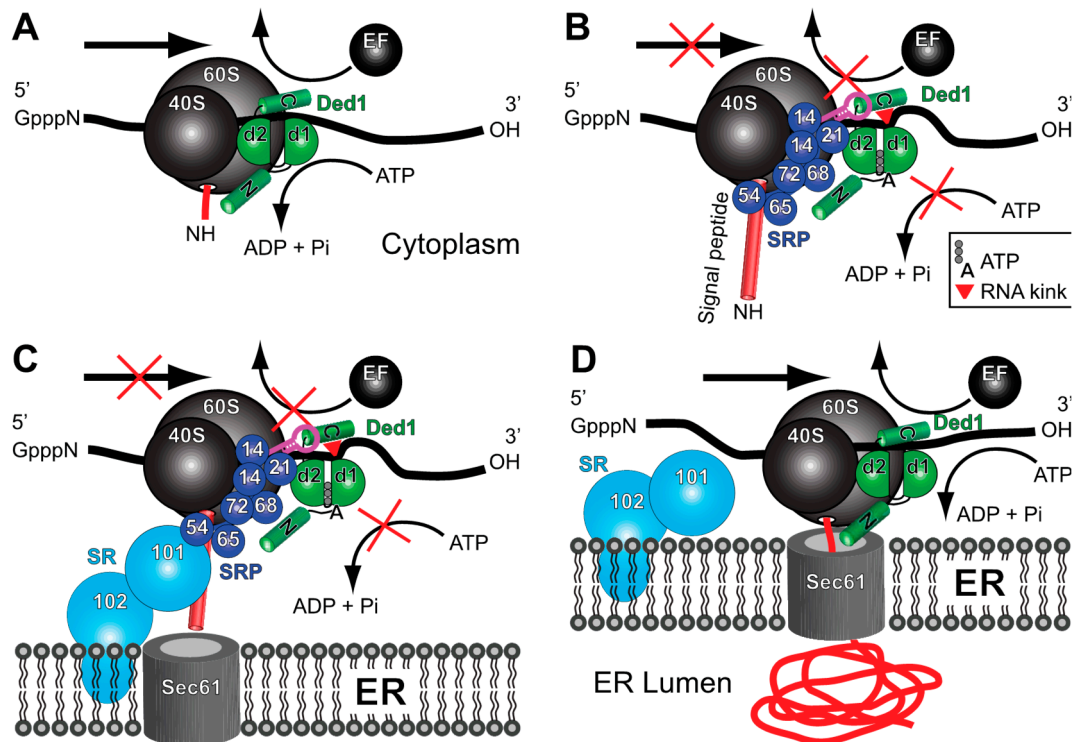


Figure 10. Model for the role of Ded1 in SRP-dependent translation. (A) Ded1 (shown in green) associates with the mRNA during translation initiation and remains attached to the mRNA in front of the ribosomes. It consists of RecA-like domains 1 (d1) and 2 (d2), an amino-terminal domain (N), and a carboxyl-terminal domain (C). The RNA-dependent ATPase activity of Ded1 is unaltered, and it is often in the “open” conformation with weak affinity for the RNA; it is able to translocate with the ribosomes during translation. The interactions with the 3′-bound Pab2 are not indicated in this cartoon. (B) The SRP (shown in blue) associates with ribosomes translating mRNAs (or undergoes conformational changes in the case of pre-bound SRP) when the signal peptide leaves the exit channel and obtains a certain length. Ded1 may help in assembling and stabilizing the complex. Conformational changes of the SRP cause SRP14 to block the entry channel and prevent the eEF2 elongation factor (EF) from binding the ribosomes, which pauses elongation. Ded1 may bind part of the Alu domain of SCR1, shown in magenta, during these conformational changes to promote SRP14 binding to the ribosomes. At the same time, SRP21 inhibits the ATPase activity of Ded1, which forms the “closed” conformation with a high affinity for the RNA. This ATP-bound form of Ded1 kinks the RNA (red triangle) on domain 1 and locks Ded1 on the RNA. This prevents the ribosomes from frameshifting (sliding) on the RNA and perhaps stabilizes the ribosome-mRNA complex to prevent the premature termination of translation. (C) The paused mRNA-ribosome complex associates with SRP receptor (SR) factors SRP101 and subsequently SRP102, which brings the mRNA-ribosome complex to the Sec61 ER translocon. (D) The SRP complex dissociates from the ribosomes, the ATPase activity of Ded1 is restored, and translation continues. Note that this model also applies to the SRP-dependent import of polypeptides with internal transmembrane domains, and it does not preclude the possibility that multiple Ded1 molecules are involved, that the SRP associates multiple times with the ribosomes during elongation, or that the SRP-associated ribosomes remain on the ER over multiple rounds of translation.

In the next step, the signal peptide binds in the hydrophobic groove of the GTPase SRP54, subsequently causing conformational changes in the SRP and its interactions with the ribosome ([39,80,82] and references therein). SRP14 bound on the Alu domain of SCR1 binds at the GTPase center located at the 40S–60S interface and thereby transiently blocks the GTPase elongation factor eEF2 from binding [36,38,39]. At the same time, SRP21 binds to Ded1 and inactivates its ATPase activity. This results in Ded1 maintaining a closed conformation that has a high affinity for the RNA but that also crimps the RNA bound on RecA domain 1; this prevents both Ded1 and the ribosomes from sliding on the mRNA by effectively clamping the mRNA (Figure 10B). Another factor other than SRP9 may play this role in metazoans. The SRP complex undergoes conformational changes during this time, and Ded1 may also bind the SCR1 RNA through its carboxyl terminus to facilitate the subsequent interactions of SRP14 with the ribosomes.

The absence of DDX3-like RNA helicases in *in vitro* reconstituted systems might explain why this pausing is often short or absent [83]. Ded1 may also stabilize the paused ribosomes to prevent premature termination or frameshifting. The paused ribosomes then associate with the peripheral-membrane GTPase SRP101 and the integral-membrane protein SRP102 that form the SRP receptor (SR) complex (Figure 10C). Once associated with the Sec61 translocon, the SRP complex undergoes further conformational changes and is either released from the ribosome or assumes an inactivated form on the ribosomes. The ATPase activity of Ded1 is restored and translation can resume (Figure 10D).

Ribosome pausing events are important for other translational events in addition to SRP-dependent protein translocation. For example, pausing is associated with co-translational protein folding, protein targeting, mRNA and protein quality control, and co-translational mRNA decay (reviewed in [84]). Ded1 (and DDX3) may be intimately associated with these events via a similar mechanism but with other associated factors besides the SRP proteins. Likewise, ribosome pausing is associated with frameshifting events (reviewed in [85,86]). Ded1 is important for L-A RNA virus replication [87] and it undergoes a -1 frameshifting event during the translation of the gag-pol gene (reviewed in [88]). Similarly, retroviruses, such as HIV-1, undergo a -1 frameshifting event during translation (reviewed in [89]). DDX3 is important for HIV-I replication, and the virions of retroviruses, in general, are enriched in 7SL RNA [23,90]. Thus, the Ded1/DDX3 subfamily of proteins may play central roles in gene expression by regulating not only translation initiation but translation elongation as well.

Finally, we note that the bacterial polypeptide-translocase SecA is a superfamily 2 “RNA helicase” that has a RecA-like core structure that is very similar to the DEAD-box proteins [91]. It is intimately associated with the SecYEG translocon and it uses ATP to drive post-translational polypeptides through the pore into the periplasm (reviewed in [25]). Recent work has shown that SecA mimics the properties of the SRP [92,93]. Thus, the use of superfamily 2 proteins for polypeptide translocation across membranes may be conserved throughout evolution. The biological roles and substrates of these proteins may not be limited to nucleic acids.

4. Materials and Methods

4.1. Constructs

4.1.1. Yeast Protein-Expression Constructs

The *DED1* constructs were derived from the YCplac111 plasmid and subcloned into the yeast plasmids 2HA-p415 and 2HA-p424 with *ADH* promoters and *LEU2* and *TRP1* markers, respectively, as previously described [94,95]. Likewise, the *ded1-F162C*, *ded1ΔC*, and *ded1-DQAD* plasmids were as previously described [13,56]. The pMW295 and pMW299 plasmids encoding the SRP proteins and SCR1 were a kind gift from Martin R. Pool [47]. They were used as templates to PCR amplify the individual genes and SCR1 RNA. The SRP genes (*SRP14*, *SRP21*, *SRP54*, *SRP68*, *SRP72*, and *SEC65*) were PCR amplified off the pMW295 or pMW299 plasmids with the corresponding SRP_up and SRP_low oligonucleotides containing 5′ *SpeI* and *NdeI* sites and 3′ *XhoI* sites [47]. The PCR products were

digested with SpeI and XhoI, gel purified, and cloned into the equivalent sites of the yeast plasmids 2HA-p415 and 2HA-p424 with *ADH* promoters and *LEU2* and *TRP1* markers, respectively [94]. *SRP14* and *SRP21* were also cloned into the *GFP_p413* plasmid [57]. The oligonucleotides used are shown in Supplementary Table S4.

SRP101 and *SRP102* were amplified off purified chromosomal DNA using oligonucleotides with BamHI and XhoI sites because of an internal SpeI site in *SRP101*. *SRP101* was PCR amplified with *SRP101_up* and *SRP101_low*. *SRP102* was PCR amplified with *SRP102_up* and *SRP102_low*. The PCR products were digested with BamHI and XhoI, gel purified, and cloned into the equivalent sites of 2HA-p424.

The *SRP14* and *SRP21* wildtype and carboxyl-terminal deletions were cloned into the p413 plasmid containing an *HIS3* marker and *ADH* promoter using an oligonucleotide complementary to the amino-terminal HA tag of the previous p415-PL-HA constructs and containing XbaI and XhoI sites [57,96]. *SRP14* was PCR amplified with *p415HA_up* and *SRP14_low*. *SRP21* was PCR amplified with *p415HA_up* and *SRP21_low*. *SRP21Δ73* was PCR amplified with *p415HA_up* and *SRP21d73_low*. The PCR products were digested with XbaI and XhoI, gel purified, and cloned into the equivalent sites of p413. The final constructs were all verified via sequencing and are shown in Supplementary Table S5.

4.1.2. *E. coli* Expression and Yeast Fluorescence Protein Constructs

Except for *SRP68* and *SEC65*, all constructs were subcloned into the NdeI and XhoI sites of pET22b. Because of internal NdeI sites, the pET19b versions of *SRP68* and *SEC65* were amplified with additional oligonucleotides. *SRP68* was PCR amplified with *SRP68_up2* and *SRP68_low2*. *SEC65* was PCR amplified with *Sec65-pET_up* and *Sec65-pET_low*. The PCR products were digested with XhoI and BamHI, gel purified, and cloned into the equivalent sites of pET19b. *SRP101* and *SRP102* were subcloned into the NdeI and XhoI sites of pET22b. *SRP21Δ73Cter* was subcloned into the NdeI and XhoI sites of pET22b.

The *GFP* and *MCHERRY* plasmids were constructed by amplifying genes off the pYM27-EGFP-KanMX4 and pFA6a-mCherry-NatNT2 plasmids, respectively. The PCR products were digested with XhoI and Sall, gel purified, and cloned into the equivalent sites of the yeast plasmids p415, p416, and p413 [97]. The *DED1*, *ded1-F162C*, and *ded1-DQAD* plasmids were subcloned into the SpeI and XhoI sites of *GFP-p415*, *p414*, and *MCHERRY_p416*. The *KAR2-RFP_YIPlac204* was a gift from Benjamin Glick. The final constructs were all verified via sequencing and are shown in Supplementary Table S5.

4.1.3. SCR1 and Actin Constructs

The oligonucleotides that were used are shown in Supplementary Table S4, where the regions of complementarity are underlined and restriction sites are shown in bold. The final constructs are listed in Supplementary Table S5.

The full-length T7-SCR1 was PCR amplified off the pMW299 plasmid [47] with the *SCR1_up2* oligonucleotide containing the T7 promoter and *SCR1-low* oligonucleotides containing 3' XhoI and DraI sites. The PCR product was digested with BamHI and XhoI, gel purified, and cloned into the equivalent sites of pUC18. The T7-SCR1ΔAlu was constructed with the *SCR1_dAlu_up* oligonucleotide containing the T7 promoter and the *SCR1_dAlu_low* oligonucleotide. The PCR product was digested with BamHI and HindIII, gel purified, and cloned into the equivalent sites of pUC18. A T7 RNA polymerase run-off transcription of the DraI-cut plasmid yielded a 522 nucleotide-long RNA with the same sequence as the endogenous SCR1 except the 5' adenosine was replaced with a guanosine to facilitate transcription. The SCR1 deletions were similarly constructed based on the secondary model of Van Nues and Brown [33]. The *SCR1ΔS1* construct replaced residues 247–371 with a UUCG tetraloop, and the *SCR1ΔAlu* construct deleted residues 1–155 and residues 454–522. The T7 RNA polymerase run-off transcriptions of the DraI-cut plasmids yielded 401 and 303 nucleotide-long RNAs, respectively. The T7-SCR1ΔS1 construct was made as fusion PCRs with two sets of oligonucleotides. The *pUC18_5'* oligonucleotide was used with *SCR1_ds1_low* and *pUC18_3'* was used with *SCR1_ds1_up*. The two

gel-purified PCR fragments were combined and PCR amplified with oligonucleotides pUC18_5' and pUC18_3'. The PCR product was digested with BamHI and HindIII, gel purified, and cloned into the equivalent sites of pUC18. These constructs are graphically shown in Supplementary Figure S5.

The actin control was a T7-promoter derivative of the previously described actin precursor RNA in the Bluescript KS(-) plasmid [98]. A T7 RNA polymerase run-off transcript of EcoRI-cut plasmid yielded a 605 nucleotide-long RNA containing, from 5' to 3', 54 nucleotides of the plasmid, 63 nucleotides of the 5' UTR, 10 nucleotides of the 5' exon, 309 nucleotides of the intron, 162 nucleotides of the 3' exon, and 7 nucleotides of the plasmid. The final constructs were all verified via sequencing and are shown in Supplementary Table S5.

4.2. Yeast Strains and Manipulations

Manipulations of yeast, including media preparation, growth conditions, transformation, and 5-FOA selection, were conducted according to standard procedures [99]. The strains used in this study are listed in Supplementary Table S6.

The yeast *GFP* clone collection was purchased from Life Technologies (Ref 95702; Carlsbad, CA, USA). The *sec61-ts* and *sec62-ts* yeast strains were a generous gift from Ron Deshaies [60]. The *KAR2-RFP* strain was created by transforming the W303 (G49), *sec61*, and *sec62* strains with EcoRV-linearized *KAR2-RFP_YIPlac204* containing the N-terminus of *KAR2* (135 bp) fused to *DsRedExpress2* with the *HDEL ER*-retention sequence. The yeast *TET*-promoter Hughes Collection strains were purchased from Dharmacon (GE Healthcare, Lafayette, CO, USA). Tetracycline-inducible strains were transformed with *GPD-DED1*, *GPD-ded1-F162C*, or the empty plasmid. Cells were grown in YPD (yeast extract, peptone, dextrose) medium or in minimal medium lacking leucine (SD-LEU), serially diluted by a factor of 10, and then plated on medium with or without 10 µg/mL of doxycycline.

4.3. Northern Blot Probes

The oligonucleotides used are listed in Supplementary Table S4. Oligonucleotides (150 pmoles) were 5' ³²P-labeled with 20 µCi of γ -³²P ATP (3000 Ci/mmol; Hartmann Analytic, Braunschweig, Germany) for 30 min at 37 °C in 50 µL volumes with 20 units of T4 PNK (New England Biolabs, Ipswich, MA, USA) in the provided reaction buffer. Reactions were heat inactivated for 20 min at 65 °C and the unincorporated radioactivity was eliminated with a G25 Illustra MicroSpin column (GE Healthcare, Chicago, IL, USA) according to the manufacturer's instructions. Labeling efficiency was determined by comparing the radioactivity of the recovered material with that retained on the column. Blots were incubated with 15 pmoles of probes overnight at 42 °C. Blots were washed two times at 42 °C with 2x SSC buffer (Euromedex, Souffelweyersheim, France) with 0.1% SDS added, washed two times with 0.2x SSC buffer with 0.1% SDS, dried, and then subjected to autoradiography with a BAS-MS imaging plate (Fujifilm, Tokyo, Japan) overnight. Exposures were revealed with a Typhoon FLA9500 phosphoimager (GE Healthcare).

4.4. In Situ Localization

To analyze the location of Ded1 relative to the ER or SRP proteins, we first used the green fluorescent protein (*GFP*)-tagged *ded1-DQAD* plasmid that was transformed into *sec61-ts* and *sec62-ts* mutant strains with the integrated *KAR2-RFP* plasmid (Supplementary Tables S5 and S6). Cells were grown in SD-LEU to an OD600 of ~0.9–1.0 (logarithmic phase) at 24 °C and then shifted to 37 °C for 15 min. We subsequently used mCherry-tagged *ded1-DQAD* plasmid that was transformed into *GFP*-tagged *SRP14* and *SRP21* expressed from the chromosome (Supplementary Tables S5 and S6). Cells were grown in SD-LEU to an OD600 of 0.95 at 30 °C. Finally, *GFP*-tagged *SRP14* or *SRP21* and mCherry-tagged *ded1-DQAD* plasmids were transformed in the *xpo1-T539C* strain [72]. Cells were grown in a minimal medium lacking histidine and uracil (SD-HIS-URA) to an OD600 of 0.4 (early logarithmic phase) at 30 °C, and then they were split into two parts: one-half was

resuspended in SD-HIS-URA and the other in SD-HIS-URA supplemented with ~200 nM of leptomycin for 1 h.

Fluorescence microscopy was performed with a Zeiss Observer.Z1 microscope (Carl Zeiss Microscopy GmbH, Oberkochen, Germany) with a 63× oil immersion objective equipped with the following filter sets: Alexa 489, filter set 10 from Zeiss for GFP (Excitation BP 450–490, Beam Splitter FT 510, Emission BP 515/65), HC-mCherry, filter set F36–508 from AHF for mCherry and RFP (Excitation BP 562/40, Beam Splitter 593, Emission BP 641/75). The images were acquired with a sCMOS ORCA FLASH 4.0 charge-coupled device camera (Hamamatsu Photonics, Shizuoka, Japan) using the Zeiss Zen 2 2012 Package Acquisition/Analysis software and processed with Zen 2 2012 (Carl Zeiss Microscopy GmbH, Göttingen, Germany) and Adobe Photoshop CS3 (Adobe, San Jose, CA, USA).

4.5. RNA Transcripts

RNAs were produced as run-off transcripts using T7 RNA polymerase and the MEGAscript kit (Ambion Thermo Fisher Scientific, Waltham, MA, USA) according to the manufacturer's instructions. In brief, reactions were performed in 20–40 µL volumes with 1–2 µg of linearized DNA and incubated for 5–6 h at 37 °C. The template was then digested with TURBO DNase; multiple reactions were combined; and the solution was diluted to 500 µL final with high-salt buffer (300 mM potassium acetate, 50 mM Tris-base, pH 8.0, 0.1 mM EDTA), extracted with an equal volume of water-saturated phenol (MP Biomedicals, Santa Ana, CA, USA), extracted with an equal volume of chloroform-isoamyl alcohol (24:1), and precipitated overnight at –20 °C with 2.5–3 volumes of ethanol. The RNA was recovered via centrifugation in an Eppendorf 5415R (Hamburg, Germany) at high speed at 4 °C for 15 min. The supernatant was discarded, the pellet washed with 300 µL of cold 70% ethanol, and the pellet dried in a SpinVac (Savant Thermo Fisher Scientific, Schwerte, Germany) for 20 min. To eliminate trace contaminants, the RNA was resuspended in 400 µL of high-salt buffer and re-ethanol precipitated at –20 °C. The pellet was recovered, washed, and dried. The final pellet was resuspended in 20 mM of Tris-base, at a pH of 7.5, with 0.1 mM of EDTA, and stored at –20 °C until needed. The concentration was determined using an absorbance at 260 nm of 32 µg/mL/cm, which was based on the calculated values of Oligo 7 software (Molecular Biology Insights, Inc., Colorado Springs, CO, USA).

4.6. Recombinant Protein Expression and Purification

Recombinant Ded1-His was expressed from the pET22b plasmid (Novagen) and purified as previously described [48]. SRP His-tagged proteins were transformed into the Rosetta (DE3) *Escherichia coli* strain. Cultures containing 500 mL of cells at OD600 of 0.5 were induced with 0.5 mM of isopropyl-1-thio-β-D-galactopyranoside (IPTG) for 1 h at 37 °C for SRP14, SEC65, and SRP101; 16 h at 16 °C for SRP68 and SRP72; and 2 h at 30 °C for SRP54 and SRP21. Cells were collected via centrifugation and the pellets were resuspended in 5 mL of lysis buffer containing 20 mM of Tris-base, at a pH of 8.0, with 0.5 M of NaCl, and the following protein-specific conditions: 20 mM of imidazole, 8 mM of β-mercaptoethanol, and 1% Triton X-100 for SRP14, SRP68, SP101, and Sec65; 20 mM of imidazole and 3 mM of β-mercaptoethanol for SRP21; 10 mM of imidazole and 3 mM of β-mercaptoethanol for SRP54; and 20 mM of imidazole and 1 mM of β-mercaptoethanol for SRP72. The equivalent of 1 mg/mL of lysozyme was added for each condition, the cells were kept on ice for 30 min, and then, the cells were lysed via sonication at 4 °C until the lysate became clear. The material was centrifuged for 40 min at 14,000 rpm in a JA-12 rotor (Beckman Coulter, Brea, CA, USA) at 4 °C and the supernatant was loaded onto a 1 mL nickel nitrilotriacetic acid–agarose column (Ni-NTA, Qiagen, Hilden, Germany) previously equilibrated with the corresponding lysis buffer. After two washes, the SRP His-tagged proteins were eluted with lysis buffer containing 150 mM of imidazole. Purified proteins were made 50% in glycerol and were quantified using the Bradford protein assay kit (Bio-Rad). Proteins were aliquoted and stored at –80 °C until needed. Recombinant

purified proteins, supplemented with SDS sample buffer, were resolved with 12% SDS polyacrylamide gel (SDS-PAGE) and stained with Coomassie Blue (Instant Blue). The properties of the different proteins are summarized in Supplementary Table S3 and the purified proteins are shown in Supplementary Figure S4.

4.7. Immunoglobulin G-Protein A-Sepharose-Bead Pull-Down Experiments

The G50 yeast strain was transformed individually with 2HA_p424 plasmids containing two amino-terminal HA tags and the genes for *SRP14*, *SRP21*, *SRP54*, *SEC65*, *SRP68*, *SRP72*, and *SRP101*. Cells were grown to an OD₆₀₀ of 0.8–1 in a minimal medium lacking tryptophan (SD-TRP), recovered via centrifugation, washed with cold water, frozen in liquid nitrogen, and stored at $-80\text{ }^{\circ}\text{C}$ until needed. The cells were resuspended in an equal volume of lysis buffer containing 20 mM of HEPES, a pH of 7.4, with 150 mM of NaCl, 5 mM of MgCl₂, 0.1 mM of EDTA, 5 mM of DTT, and 1x protease inhibitor cocktail (Roche cOmplete EDTA-Free). An equal volume of 425–600 μm glass beads (Sigma-Aldrich, St. Louis, MO, USA) was added and the cells were broken via vortexing in a FastPrep-24 (MP Biomedicals) at $4\text{ }^{\circ}\text{C}$ with four cycles of 30 s and 5 min rests. The cell debris was removed via centrifugation for 5 min at 6000 rpm in an Eppendorf 5415R centrifuge at $4\text{ }^{\circ}\text{C}$. The lysates were further clarified via centrifugation two to three times at 13,000 rpm for 10 min each at $4\text{ }^{\circ}\text{C}$. The protein concentrations were determined with a Bio-Rad Protein Assay kit according to the manufacturer's instructions using bovine serum albumin (BSA) as a standard.

Protein A-Sepharose CL-4B beads (GE Healthcare) were prepared by first washing them twice in IPP150 buffer containing 20 mM of Tris-base, at a pH of 7.4, with 150 mM of NaCl, 0.1% Triton-X100, and 1 mM of MgCl₂. Then, 50 μL of beads was incubated overnight by mixing in 10 volumes of IPP150 buffer at $4\text{ }^{\circ}\text{C}$ with 0.4 mg/mL of BSA, 0.4 mg/mL of heparin, and 20 μL of serum containing Ded1, SRP21, HA (Covalab, Bron, France), or pre-immune immunoglobulin G (IgG). The beads were washed three times with 800 μL of 1x PBS and then mixed at $4\text{ }^{\circ}\text{C}$ for 2 h with G50 extracts containing 300 μg of protein and 10 volumes of 1x PBS buffer supplemented with BSA and heparin. The beads were washed three times with 800 μL of 1x PBS, and the bound proteins were eluted twice with 300 μL of 0.1 M of glycine, with a pH of 2.3 for 15 min at $4\text{ }^{\circ}\text{C}$ with mixing. The pH of the eluted proteins was then adjusted to pH ~ 7 with NaOH.

4.8. Other Pull-Down Experiments

Protein A-Sepharose beads were prepared as described above. Ded1 or SRP21 IgG were crosslinked to beads with 0.2% glutaraldehyde as described previously [100] and were rigorously washed with 1x PBS. The equivalent of 4–6 μg of purified Ded1 and SRP proteins were incubated with 300 μL of 1x PSB supplemented with 2 mM of MgCl₂ for 45 min at $30\text{ }^{\circ}\text{C}$. Fifteen μL of Protein A-Sepharose beads was directly added to the protein mixture and mixed via rotation for 1 h at $18\text{ }^{\circ}\text{C}$. Prior to elution, beads were washed three times with 1x PBS. The bound proteins were eluted with 30 μL of glycine, at a pH of 2.3, for 15 min at $4\text{ }^{\circ}\text{C}$ on a rotating wheel platform. The acidity of the reaction was neutralized by adding NaOH. Co-immunoprecipitated purified proteins, supplemented with SDS sample buffer, were resolved on a 12% SDS-PAGE and stained with Coomassie Blue.

4.9. Western Blot Analysis

The eluted proteins were concentrated by making the solution 150 $\mu\text{g}/\text{mL}$ in sodium deoxycholate and the proteins precipitated with 15%, final, of trichloroacetic acid (TCA) for 16 h at $4\text{ }^{\circ}\text{C}$. The solution was centrifuged for 30 min in an Eppendorf 5415R centrifuge at high speed, and the recovered pellet was washed with cold acetone, dried, and resuspended in loading buffer containing 50 mM of Tris-base, with a pH of 6.8, with 2% sodium dodecyl sulfate (SDS), 1% β -mercaptoethanol, 0.02% bromophenol blue, and 10% glycerol. The eluted proteins were separated on SDS-Laemmli gels, transferred to Amersham Protran nitrocellulose membranes (GE Healthcare Life Science), and probed with primary IgG

against Ded1, SRP21, Sec65, or HA. The anti-Sec65 antibody was a generous gift from Martin R. Pool. Horseradish peroxidase-conjugated anti-rabbit (for Ded1, Sec65, SRP21; Covalab) and anti-mouse (for HA; Covalab) were used as secondary antibodies, and the signals were revealed with a Clarity Western ECL Substrate kit (Bio-Rad) using a Bio-Rad ChemiDoc XRS+ and Image Lab 5.2 software. The Ded1-IgG and SRP21-IgG were produced with Covalab using purified recombinant Ded1 or SRP21, respectively.

4.10. Reverse-Transcriptase PCR

Samples were digested with proteinase K by adding 1 mg/mL of proteinase K (Sigma #P2308-100MG), 1% triton X-100, 0.5% SDS, and 5 mM of CaCl₂ in an Eppendorf Thermomixer Comfort (15 s 1000 rpm, 90 s rest) at 55 °C for 35 min. Total RNA (input condition) and RNA from the eluate were recovered via the addition of 0.3 M of potassium acetate, extracted with an equal volume of water-saturated phenol, extracted twice with an equal volume of chloroform-isoamyl alcohol (24:1), and then ethanol precipitated overnight at −20 °C. The RNA pellets from the ethanol precipitations were resuspended in 20 µL of nuclease-free water. RNA was reverse transcribed with the Superscript III kit (Invitrogen, Carlsbad, CA, USA) according to the manufacturer's instructions. In brief, 4.6 µL of the resuspended Ded1, pre-immune IgG pull-downs, and 0.5 µg of total yeast RNA were combined with 1 pmole of the 3' primers specific for SCR1, PGK1, or RPL20B RNAs (Supplementary Table S4). The reactions were heated to 50 °C for 5 min and then 10 mM of DTT, 0.75 µL of Superscript III Reverse Transcriptase (RT), 1x final of RT buffer, and 3 mM final of dNTPs were added. The reactions were incubated for 90 min at 50 °C. The RNAs were hydrolyzed by adding 40 µL of a solution with 150 mM of KOH and 20 mM of Tris-base and incubating at 90 °C for 10 min. The solution was neutralized by adding 40 µL of 150 mM HCl. The PCR amplification was performed with 10 µL of the reverse-transcriptase product in a 50 µL PCR mix containing 1 unit of Phusion High-Fidelity DNA polymerase (New England Biolabs), 1x HF Phusion buffer, 0.2 mM of dNTPs, and 0.5 pmoles of the respective gene-specific 5' and 3' primers (Supplementary Table S4). PCR reactions were conducted for 25 cycles in a Bio-Rad T100 Thermal Cycler. PCR products were purified with a NucleoSpin Gel and PCR Clean-up kit (Macherey-Nagel, Düren, Germany), eluted with 50 µL of elution buffer, and 5 µL aliquots were analyzed with agarose loading buffer on a 2% agarose gel containing ethidium bromide.

4.11. In Vitro RNA-Dependent ATPase Activities

The ATPase assays were based on a colorimetric assay using molybdate-Malachite green as previously described [48]. We typically used 23 nM of SCR1 or actin RNA and 0.14 µg/µL of whole yeast RNA (Roche) that was purified on a DEAE-Sephadex column to remove inhibitors. For the latter RNA, fractions from elution with increasing concentrations of NaCl were assayed with purified Ded1, and the most active fractions were combined, concentrated through ethanol precipitation, and subsequently used in the assays. The poly(A) RNA was from Sigma. Assays were performed in a reaction mix with 20 mM of Tris-base, at a pH of 7.5, with 50 mM of potassium acetate, 5 mM of magnesium acetate, 0.1 µg/µL of BSA, and 2 mM of DTT. Purified proteins and RNAs were pre-incubated for 30 min at 30 °C to equilibrate the different components. We used the Ded1-K192A (GAT) mutant in motif I as a negative control as it had no detectable ATPase activity [48]. Reactions were started by adding 1 mM final of ATP and taking aliquots over the time course. The reactions were stopped by making the solutions approximately 60 mM final in EDTA. The Malachite green solution was added as previously described [48] and the absorption was measured with a Tecan NanoQuant Infinite M200Pro microtiter plate reader (Männedorf, Switzerland) at 630 nm. Enzymatic reaction velocities were determined by a linear regression fit over the initial linear phase of the reaction with five data points over a time course of 45 min using optimized protein concentrations. We used a serial dilution of Phosphate Phosphorous Standard for IC (Fluka Sigma-Aldrich) for each experiment to

determine the corresponding phosphate concentration from the absorption. Experimental data were analyzed with Kaleidagraph 4.5.2 software (Synergy, Reading, PA, USA).

4.12. Electrophoretic Mobility-Shift Assays

An EMSA-agarose technique was used as previously described with minor modifications [101]. Briefly, the assay was performed with 0.150 μ M of SCR1 or actin RNA and variable concentrations of the indicated proteins, which were incubated together in 1x EMSA buffer (20 mM of Tris-base, at a pH of 8.8, with 70 mM of KOAc, 2 mM of MgCl₂, 10 μ g/ μ L of BSA, and 1 mM of DTT) for 15 min at 30 °C in the presence or absence of 5 mM of AMP-PNP or ATP in a volume of 8 μ L. Two μ L of 30% glycerol was added to the samples, and they were loaded onto 0.75 mm thick, 1% agarose (Molecular Biology Grade) gels containing 1x TBE buffer (45 mM of Tris-base, 45 mM of boric acid, at a pH of 8.8, and 2 mM of EDTA; Sigma) and ~0.016 μ g/mL of ethidium bromide. Gels were run in a mini-plus horizontal electrophoresis (Scie-Plas) in 1x TBE buffer at 220 V for ~13 min at 4 °C and were imaged with a Gel Doc XR+ (Bio-RAD) and Quantity One 4.6.9 software (Bio-Rad).

Supplementary Materials: The following supporting information can be downloaded at <https://www.mdpi.com/article/10.3390/molecules29122944/s1>: Supplementary Table S1: Sucrose gradients fractions; nano-LC ESI MS/MS analysis. Supplementary Table S2: Ded1-IgG Pull-down of sucrose gradients fractions; nano-LC ESI MS/MS analysis. Supplementary Table S3: Protein characteristics. Supplementary Table S4: Oligonucleotides used in this study. Supplementary Table S5: Constructs used in this study. Supplementary Table S6: Yeast and bacterial strains used in this study. Supplementary Figure S1: Heat map of the recovered PAR-CLIP fragments. Supplementary Figure S2: Multiple-copy suppression of the ded1-F162C cold-sensitive phenotype. Supplementary Figure S3: Phenotypes of proteins expressed with tetracycline promoters. Supplementary Figure S4: Purified His-tagged recombinant proteins. Supplementary Figure S5: SCR1 deletion constructs. Supplementary Figure S6: Ded1 and SRP21 bound SCR1 and actin separately. Refs. [13,32,33,47,48,56,60,72,74,94–98,102] are cited in Supplementary Materials.

Author Contributions: Conceptualization, N.K.T., H.Y.-A., N.B.-T. and J.B.; methodology, N.K.T., H.Y.-A., N.B.-T., A.L.S., E.H., M.M. and J.B.; validation, N.K.T., H.Y.-A., N.B.-T. and J.B.; formal analysis, N.K.T., H.Y.-A. and J.B.; investigation, N.K.T., H.Y.-A., N.B.-T. and J.B.; resources, N.K.T., N.B.-T. and J.B.; data curation, N.K.T., H.Y.-A., N.B.-T. and J.B.; writing—original draft preparation, N.K.T., H.Y.-A., N.B.-T. and J.B.; writing—review and editing, N.K.T., H.Y.-A., N.B.-T. and J.B.; visualization, N.K.T., H.Y.-A., N.B.-T. and J.B.; supervision, N.K.T. and J.B.; project administration, N.K.T.; funding acquisition, N.K.T. All authors have read and agreed to the published version of the manuscript.

Funding: This work was supported by the Centre National de la Recherche Scientifique; HeliDEAD grant [grant number ANR-13-BSV8-0009-01 to NKT] from the Agence Nationale de la Recherche; and the Initiative d'Excellence program from the French State grant DYNAMO [grant number ANR-11-LABX-0011-01].

Institutional Review Board Statement: Not applicable.

Informed Consent Statement: Not applicable.

Data Availability Statement: Sequencing data can be retrieved using GEO accession number GSE228828. Additional data are available upon request.

Acknowledgments: We thank Caroline Lacoux and Stéphanie Ørum for helpful discussions; Martin R Pool for the Sec65 IgG and for the pMW295 and pMW299 SRP plasmids; Benjamin Glick for the KAR2-RFP_YIPlac204; Jiří Hašek for the pFA6a-mCherry-NatNT2 plasmid; Michael Lisby and Rodney Rothstein for the G49 and G50 yeast strains; and Claude Thermes, Yves Daubenton, Erwin Van Dijk, Yan Jaszczyszyn, Pauline Francois, Marina Cavaiuolo, and Benoist Laurent for their help with RNAseq.

Conflicts of Interest: The authors declare no conflicts of interest. The funders had no role in the design of the study; in the collection, analyses, or interpretation of data; in the writing of the manuscript; or in the decision to publish the results.

References

1. Cordin, O.; Banroques, J.; Tanner, N.K.; Linder, P. The DEAD-box protein family of RNA helicases. *Gene* **2006**, *367*, 17–37. [[CrossRef](#)] [[PubMed](#)]
2. Linder, P.; Jankowsky, E. From unwinding to clamping—The DEAD box RNA helicase family. *Nat. Rev. Mol. Cell Biol.* **2011**, *12*, 505–516. [[CrossRef](#)] [[PubMed](#)]
3. Putnam, A.A.; Jankowsky, E. DEAD-box helicases as integrators of RNA, nucleotide and protein binding. *Biochim. Biophys. Acta* **2013**, *1829*, 884–893. [[CrossRef](#)] [[PubMed](#)]
4. Byrd, A.K.; Raney, K.D. Superfamily 2 helicases. *Front. Biosci. Landmark Ed.* **2012**, *17*, 2070–2088. [[CrossRef](#)] [[PubMed](#)]
5. Fairman-Williams, M.E.; Guenther, U.P.; Jankowsky, E. SF1 and SF2 helicases: Family matters. *Curr. Opin. Struct. Biol.* **2010**, *20*, 313–324. [[CrossRef](#)] [[PubMed](#)]
6. Raj, S.; Bagchi, D.; Orero, J.V.; Banroques, J.; Tanner, N.K.; Croquette, V. Mechanistic characterization of the DEAD-box RNA helicase Ded1 from yeast as revealed by a novel technique using single-molecule magnetic tweezers. *Nucleic Acids Res.* **2019**, *47*, 3699–3710. [[CrossRef](#)] [[PubMed](#)]
7. Ozgur, S.; Buchwald, G.; Falk, S.; Chakrabarti, S.; Prabu, J.R.; Conti, E. The conformational plasticity of eukaryotic RNA-dependent ATPases. *FEBS J.* **2015**, *282*, 850–863. [[CrossRef](#)] [[PubMed](#)]
8. Liu, F.; Putnam, A.A.; Jankowsky, E. DEAD-box helicases form nucleotide-dependent, long-lived complexes with RNA. *Biochemistry* **2014**, *53*, 423–433. [[CrossRef](#)]
9. Sharma, D.; Jankowsky, E. The Ded1/DDX3 subfamily of DEAD-box RNA helicases. *Crit. Rev. Biochem. Mol. Biol.* **2014**, *49*, 343–360. [[CrossRef](#)] [[PubMed](#)]
10. Chang, T.C.; Liu, W.S. The molecular evolution of PL10 homologs. *BMC Evol. Biol.* **2010**, *10*, 127. [[CrossRef](#)]
11. Tarn, W.Y.; Chang, T.H. The current understanding of Ded1p/DDX3 homologs from yeast to human. *RNA Biol.* **2009**, *6*, 17–20. [[CrossRef](#)] [[PubMed](#)]
12. Rosner, A.; Rinkevich, B. The DDX3 subfamily of the DEAD box helicases: Divergent roles as unveiled by studying different organisms and in vitro assays. *Curr. Med. Chem.* **2007**, *14*, 2517–2525. [[CrossRef](#)] [[PubMed](#)]
13. Senissar, M.; Le Saux, A.; Belgareh-Touze, N.; Adam, C.; Banroques, J.; Tanner, N.K. The DEAD-box helicase Ded1 from yeast is an mRNP cap-associated protein that shuttles between the cytoplasm and nucleus. *Nucleic Acids Res.* **2014**, *42*, 10005–10022. [[CrossRef](#)] [[PubMed](#)]
14. Gupta, N.; Lorsch, J.R.; Hinnebusch, A.G. Yeast Ded1 promotes 48S translation pre-initiation complex assembly in an mRNA-specific and eIF4F-dependent manner. *eLife* **2018**, *7*, e38892. [[CrossRef](#)] [[PubMed](#)]
15. Dever, T.E.; Kinzy, T.G.; Pavitt, G.D. Mechanism and Regulation of Protein Synthesis in *Saccharomyces cerevisiae*. *Genetics* **2016**, *203*, 65–107. [[CrossRef](#)]
16. Gulay, S.; Gupta, N.; Lorsch, J.R.; Hinnebusch, A.G. Distinct interactions of eIF4A and eIF4E with RNA helicase Ded1 stimulate translation in vivo. *eLife* **2020**, *9*, e58243. [[CrossRef](#)]
17. Aryanpur, P.P.; Regan, C.A.; Collins, J.M.; Mittelmeier, T.M.; Renner, D.M.; Vergara, A.M.; Brown, N.P.; Bolger, T.A. Gle1 Regulates RNA Binding of the DEAD-Box Helicase Ded1 in Its Complex Role in Translation Initiation. *Mol. Cell. Biol.* **2017**, *37*, e00139-17. [[CrossRef](#)]
18. Hauk, G.; Bowman, G.D. Formation of a Trimeric Xpo1-Ran[GTP]-Ded1 Exportin Complex Modulates ATPase and Helicase Activities of Ded1. *PLoS ONE* **2015**, *10*, e0131690. [[CrossRef](#)]
19. Ivanov, P.; Kedersha, N.; Anderson, P. Stress Granules and Processing Bodies in Translational Control. *Cold Spring Harb. Perspect. Biol.* **2019**, *11*, a032813. [[CrossRef](#)]
20. Youn, J.Y.; Dyakov, B.J.A.; Zhang, J.; Knight, J.D.R.; Vernon, R.M.; Forman-Kay, J.D.; Gingras, A.C. Properties of Stress Granule and P-Body Proteomes. *Mol. Cell* **2019**, *76*, 286–294. [[CrossRef](#)]
21. Guzikowski, A.R.; Chen, Y.S.; Zid, B.M. Stress-induced mRNP granules: Form and function of processing bodies and stress granules. *Wiley Interdiscip. Rev. RNA* **2019**, *10*, e1524. [[CrossRef](#)] [[PubMed](#)]
22. Hondele, M.; Sachdev, R.; Heinrich, S.; Wang, J.; Vallotton, P.; Fontoura, B.M.A.; Weis, K. DEAD-box ATPases are global regulators of phase-separated organelles. *Nature* **2019**, *573*, 144–148. [[CrossRef](#)] [[PubMed](#)]
23. Soto-Rifo, R.; Ohlmann, T. The role of the DEAD-box RNA helicase DDX3 in mRNA metabolism. *Wiley Interdiscip. Rev. RNA* **2013**, *4*, 369–385. [[CrossRef](#)] [[PubMed](#)]
24. Yeter-Alat, H.; Belgareh-Touzé, N.; Huvelle, E.; Banroques, J.; Tanner, N.K. The DEAD-Box RNA Helicase Ded1 Is Associated with Translating Ribosomes. *Genes* **2023**, *14*, 1566. [[CrossRef](#)] [[PubMed](#)]
25. Rapoport, T.A.; Li, L.; Park, E. Structural and Mechanistic Insights into Protein Translocation. *Annu. Rev. Cell Dev. Biol.* **2017**, *33*, 369–390. [[CrossRef](#)] [[PubMed](#)]
26. Wild, K.; Becker, M.M.M.; Kempf, G.; Sinning, I. Structure, dynamics and interactions of large SRP variants. *Biol. Chem.* **2019**, *401*, 63–80. [[CrossRef](#)] [[PubMed](#)]
27. Cui, X.A.; Palazzo, A.F. Localization of mRNAs to the endoplasmic reticulum. *Wiley Interdiscip. Rev. RNA* **2014**, *5*, 481–492. [[CrossRef](#)]
28. Akopian, D.; Shen, K.; Zhang, X.; Shan, S.O. Signal recognition particle: An essential protein-targeting machine. *Annu. Rev. Biochem.* **2013**, *82*, 693–721. [[CrossRef](#)]

29. Pool, M.R. Signal recognition particles in chloroplasts, bacteria, yeast and mammals (review). *Mol. Membr. Biol.* **2005**, *22*, 3–15. [[CrossRef](#)]
30. Rosenblad, M.A.; Larsen, N.; Samuelsson, T.; Zwieb, C. Kinship in the SRP RNA family. *RNA Biol.* **2009**, *6*, 508–516. [[CrossRef](#)]
31. Massenet, S. In vivo assembly of eukaryotic signal recognition particle: A still enigmatic process involving the SMN complex. *Biochimie* **2019**, *164*, 99–104. [[CrossRef](#)] [[PubMed](#)]
32. Zwieb, C.; van Nues, R.W.; Rosenblad, M.A.; Brown, J.D.; Samuelsson, T. A nomenclature for all signal recognition particle RNAs. *RNA* **2005**, *11*, 7–13. [[CrossRef](#)] [[PubMed](#)]
33. Van Nues, R.W.; Brown, J.D. *Saccharomyces* SRP RNA secondary structures: A conserved S-domain and extended Alu-domain. *RNA* **2004**, *10*, 75–89. [[CrossRef](#)] [[PubMed](#)]
34. Nyathi, Y.; Wilkinson, B.M.; Pool, M.R. Co-translational targeting and translocation of proteins to the endoplasmic reticulum. *Biochim. Biophys. Acta* **2013**, *1833*, 2392–2402. [[CrossRef](#)] [[PubMed](#)]
35. Strub, K.; Fornallaz, M.; Bui, N. The Alu domain homolog of the yeast signal recognition particle consists of an Srp14p homodimer and a yeast-specific RNA structure. *RNA* **1999**, *5*, 1333–1347. [[CrossRef](#)] [[PubMed](#)]
36. Mason, N.; Ciuffo, L.F.; Brown, J.D. Elongation arrest is a physiologically important function of signal recognition particle. *EMBO J.* **2000**, *19*, 4164–4174. [[CrossRef](#)] [[PubMed](#)]
37. Rosenblad, M.A.; Zwieb, C.; Samuelsson, T. Identification and comparative analysis of components from the signal recognition particle in protozoa and fungi. *BMC Genom.* **2004**, *5*, 5. [[CrossRef](#)] [[PubMed](#)]
38. Halic, M.; Becker, T.; Pool, M.R.; Spahn, C.M.; Grassucci, R.A.; Frank, J.; Beckmann, R. Structure of the signal recognition particle interacting with the elongation-arrested ribosome. *Nature* **2004**, *427*, 808–814. [[CrossRef](#)]
39. Bousset, L.; Mary, C.; Brooks, M.A.; Scherrer, A.; Strub, K.; Cusack, S. Crystal structure of a signal recognition particle Alu domain in the elongation arrest conformation. *RNA* **2014**, *20*, 1955–1962. [[CrossRef](#)]
40. Wild, K.; Juare, K.D.; Soni, K.; Shanmuganathan, V.; Hendricks, A.; Segnitz, B.; Beckmann, R.; Sinning, I. Reconstitution of the human SRP system and quantitative and systematic analysis of its ribosome interactions. *Nucleic Acids Res.* **2019**, *47*, 3184–3196. [[CrossRef](#)]
41. Ashe, M.P.; De Long, S.K.; Sachs, A.B. Glucose depletion rapidly inhibits translation initiation in yeast. *Mol. Biol. Cell* **2000**, *11*, 833–848. [[CrossRef](#)] [[PubMed](#)]
42. Lui, J.; Campbell, S.G.; Ashe, M.P. Inhibition of translation initiation following glucose depletion in yeast facilitates a rationalization of mRNA content. *Biochem. Soc. Trans.* **2010**, *38*, 1131–1136. [[CrossRef](#)] [[PubMed](#)]
43. Janapala, Y.; Preiss, T.; Shirokikh, N.E. Control of Translation at the Initiation Phase During Glucose Starvation in Yeast. *Int. J. Mol. Sci.* **2019**, *20*, 4043. [[CrossRef](#)]
44. Shuman, S. Transcriptional interference at tandem lncRNA and protein-coding genes: An emerging theme in regulation of cellular nutrient homeostasis. *Nucleic Acids Res.* **2020**, *48*, 8243–8254. [[CrossRef](#)]
45. Ho, B.; Baryshnikova, A.; Brown, G.W. Unification of Protein Abundance Datasets Yields a Quantitative *Saccharomyces cerevisiae* Proteome. *Cell Syst.* **2018**, *6*, 192–205.e193. [[CrossRef](#)] [[PubMed](#)]
46. Guenther, U.P.; Weinberg, D.E.; Zubradt, M.M.; Tedeschi, F.A.; Stawicki, B.N.; Zagore, L.L.; Brar, G.A.; Licatalosi, D.D.; Bartel, D.P.; Weissman, J.S.; et al. The helicase Ded1p controls use of near-cognate translation initiation codons in 5' UTRs. *Nature* **2018**, *559*, 130–134. [[CrossRef](#)] [[PubMed](#)]
47. Willer, M.; Jermy, A.J.; Steel, G.J.; Garside, H.J.; Carter, S.; Stirling, C.J. An in vitro assay using overexpressed yeast SRP demonstrates that cotranslational translocation is dependent upon the J-domain of Sec63p. *Biochemistry* **2003**, *42*, 7171–7177. [[CrossRef](#)]
48. Cordin, O.; Tanner, N.K.; Doere, M.; Linder, P.; Banroques, J. The newly discovered Q motif of DEAD-box RNA helicases regulates RNA-binding and helicase activity. *EMBO J.* **2004**, *23*, 2478–2487. [[CrossRef](#)] [[PubMed](#)]
49. Brown, J.D.; Hann, B.C.; Medzihradzky, K.F.; Niwa, M.; Burlingame, A.L.; Walter, P. Subunits of the *Saccharomyces cerevisiae* signal recognition particle required for its functional expression. *EMBO J.* **1994**, *13*, 4390–4400. [[CrossRef](#)]
50. Hann, B.C.; Walter, P. The signal recognition particle in *S. cerevisiae*. *Cell* **1991**, *67*, 131–144. [[CrossRef](#)] [[PubMed](#)]
51. Stirling, C.J.; Hewitt, E.W. The *S. cerevisiae* SEC65 gene encodes a component of yeast signal recognition particle with homology to human SRP19. *Nature* **1992**, *356*, 534–537. [[CrossRef](#)] [[PubMed](#)]
52. Ogg, S.C.; Poritz, M.A.; Walter, P. Signal recognition particle receptor is important for cell growth and protein secretion in *Saccharomyces cerevisiae*. *Mol. Biol. Cell* **1992**, *3*, 895–911. [[CrossRef](#)]
53. Mutka, S.C.; Walter, P. Multifaceted physiological response allows yeast to adapt to the loss of the signal recognition particle-dependent protein-targeting pathway. *Mol. Biol. Cell* **2001**, *12*, 577–588. [[CrossRef](#)] [[PubMed](#)]
54. Hughes, T.R.; Marton, M.J.; Jones, A.R.; Roberts, C.J.; Stoughton, R.; Armour, C.D.; Bennett, H.A.; Coffey, E.; Dai, H.; He, Y.D.; et al. Functional discovery via a compendium of expression profiles. *Cell* **2000**, *102*, 109–126. [[CrossRef](#)] [[PubMed](#)]
55. Beckham, C.; Hilliker, A.; Cziko, A.M.; Noueir, A.; Ramaswami, M.; Parker, R. The DEAD-box RNA helicase Ded1p affects and accumulates in *Saccharomyces cerevisiae* P-bodies. *Mol. Biol. Cell* **2008**, *19*, 984–993, Erratum in *Mol. Biol. Cell* **2012**, *23*, 2818. [[CrossRef](#)]
56. Banroques, J.; Cordin, O.; Doère, M.; Linder, P.; Tanner, N.K. Analyses of the functional regions of DEAD-box RNA "helicases" with deletion and chimera constructs tested in vivo and in vitro. *J. Mol. Biol.* **2011**, *413*, 451–472. [[CrossRef](#)] [[PubMed](#)]

57. Mumberg, D.; Muller, R.; Funk, M. Yeast vectors for the controlled expression of heterologous proteins in different genetic backgrounds. *Gene* **1995**, *156*, 119–122. [[CrossRef](#)]
58. Chuang, R.Y.; Weaver, P.L.; Liu, Z.; Chang, T.H. Requirement of the DEAD-Box protein Ded1p for messenger RNA translation. *Science* **1997**, *275*, 1468–1471. [[CrossRef](#)]
59. Iserman, C.; Desroches Altamirano, C.; Jegers, C.; Friedrich, U.; Zarin, T.; Fritsch, A.W.; Mittasch, M.; Domingues, A.; Hersemann, L.; Jahnel, M.; et al. Condensation of Ded1p Promotes a Translational Switch from Housekeeping to Stress Protein Production. *Cell* **2020**, *181*, 818–831.e819. [[CrossRef](#)]
60. Deshaies, R.J.; Schekman, R. A yeast mutant defective at an early stage in import of secretory protein precursors into the endoplasmic reticulum. *J. Cell Biol.* **1987**, *105*, 633–645. [[CrossRef](#)]
61. Deshaies, R.J.; Schekman, R. SEC62 encodes a putative membrane protein required for protein translocation into the yeast endoplasmic reticulum. *J. Cell Biol.* **1989**, *109*, 2653–2664. [[CrossRef](#)] [[PubMed](#)]
62. Nishikawa, S.I.; Fewell, S.W.; Kato, Y.; Brodsky, J.L.; Endo, T. Molecular chaperones in the yeast endoplasmic reticulum maintain the solubility of proteins for retrotranslocation and degradation. *J. Cell Biol.* **2001**, *153*, 1061–1070. [[CrossRef](#)] [[PubMed](#)]
63. West, M.; Zurek, N.; Hoenger, A.; Voeltz, G.K. A 3D analysis of yeast ER structure reveals how ER domains are organized by membrane curvature. *J. Cell Biol.* **2011**, *193*, 333–346. [[CrossRef](#)] [[PubMed](#)]
64. Babu, M.; Vlasblom, J.; Pu, S.; Guo, X.; Graham, C.; Bean, B.D.; Burston, H.E.; Vizeacoumar, F.J.; Snider, J.; Phanse, S.; et al. Interaction landscape of membrane-protein complexes in *Saccharomyces cerevisiae*. *Nature* **2012**, *489*, 585–589. [[CrossRef](#)] [[PubMed](#)]
65. Wild, K.; Sinning, I. RNA gymnastics in mammalian signal recognition particle assembly. *RNA Biol.* **2014**, *11*, 1330–1334. [[CrossRef](#)] [[PubMed](#)]
66. Leung, E.; Brown, J.D. Biogenesis of the signal recognition particle. *Biochem. Soc. Trans.* **2010**, *38*, 1093–1098. [[CrossRef](#)] [[PubMed](#)]
67. Ciufu, L.F.; Brown, J.D. Nuclear export of yeast signal recognition particle lacking Srp54p by the Xpo1p/Crm1p NES-dependent pathway. *Curr. Biol. CB* **2000**, *10*, 1256–1264. [[CrossRef](#)]
68. Grosshans, H.; Deinert, K.; Hurt, E.; Simos, G. Biogenesis of the signal recognition particle (SRP) involves import of SRP proteins into the nucleolus, assembly with the SRP-RNA, and Xpo1p-mediated export. *J. Cell Biol.* **2001**, *153*, 745–762. [[CrossRef](#)]
69. Baßler, J.; Hurt, E. Eukaryotic Ribosome Assembly. *Annu. Rev. Biochem.* **2019**, *88*, 281–306. [[CrossRef](#)]
70. Yedavalli, V.S.; Neuveut, C.; Chi, Y.H.; Kleiman, L.; Jeang, K.T. Requirement of DDX3 DEAD box RNA helicase for HIV-1 Rev-RRE export function. *Cell* **2004**, *119*, 381–392. [[CrossRef](#)]
71. Nishi, K.; Yoshida, M.; Fujiwara, D.; Nishikawa, M.; Horinouchi, S.; Beppu, T. Leptomycin B targets a regulatory cascade of crm1, a fission yeast nuclear protein, involved in control of higher order chromosome structure and gene expression. *J. Biol. Chem.* **1994**, *269*, 6320–6324. [[CrossRef](#)] [[PubMed](#)]
72. Neville, M.; Rosbash, M. The NES-Crm1p export pathway is not a major mRNA export route in *Saccharomyces cerevisiae*. *EMBO J.* **1999**, *18*, 3746–3756. [[CrossRef](#)] [[PubMed](#)]
73. Hann, B.C.; Stirling, C.J.; Walter, P. SEC65 gene product is a subunit of the yeast signal recognition particle required for its integrity. *Nature* **1992**, *356*, 532–533. [[CrossRef](#)] [[PubMed](#)]
74. Iost, I.; Dreyfus, M.; Linder, P. Ded1p, a DEAD-box protein required for translation initiation in *Saccharomyces cerevisiae*, is an RNA helicase. *J. Biol. Chem.* **1999**, *274*, 17677–17683. [[CrossRef](#)] [[PubMed](#)]
75. Banroques, J.; Cordin, O.; Doère, M.; Linder, P.; Tanner, N.K. A conserved phenylalanine of motif IV in superfamily 2 helicases is required for cooperative, ATP-dependent binding of RNA substrates in DEAD-box proteins. *Mol. Cell. Biol.* **2008**, *28*, 3359–3371. [[CrossRef](#)] [[PubMed](#)]
76. Valentin-Vega, Y.A.; Wang, Y.D.; Parker, M.; Patmore, D.M.; Kanagaraj, A.; Moore, J.; Rusch, M.; Finkelstein, D.; Ellison, D.W.; Gilbertson, R.J.; et al. Cancer-associated DDX3X mutations drive stress granule assembly and impair global translation. *Sci. Rep.* **2016**, *6*, 25996. [[CrossRef](#)] [[PubMed](#)]
77. Schäfer, T.; Strauss, D.; Petfalski, E.; Tollervey, D.; Hurt, E. The path from nucleolar 90S to cytoplasmic 40S pre-ribosomes. *EMBO J.* **2003**, *22*, 1370–1380. [[CrossRef](#)] [[PubMed](#)]
78. Mayr, C. What Are 3' UTRs Doing? *Cold Spring Harb. Perspect. Biol.* **2019**, *11*, a034728. [[CrossRef](#)]
79. Chartron, J.W.; Hunt, K.C.; Frydman, J. Cotranslational signal-independent SRP preloading during membrane targeting. *Nature* **2016**, *536*, 224–228. [[CrossRef](#)]
80. Voorhees, R.M.; Hegde, R.S. Toward a structural understanding of co-translational protein translocation. *Curr. Opin. Cell Biol.* **2016**, *41*, 91–99. [[CrossRef](#)]
81. Wolin, S.L.; Walter, P. Signal recognition particle mediates a transient elongation arrest of preprolactin in reticulocyte lysate. *J. Cell Biol.* **1989**, *109*, 2617–2622. [[CrossRef](#)] [[PubMed](#)]
82. Flores, J.K.; Ataide, S.F. Structural Changes of RNA in Complex with Proteins in the SRP. *Front. Mol. Biosci.* **2018**, *5*, 7. [[CrossRef](#)] [[PubMed](#)]
83. Voorhees, R.M.; Hegde, R.S. Structures of the scanning and engaged states of the mammalian SRP-ribosome complex. *eLife* **2015**, *4*, e07975. [[CrossRef](#)]
84. Collart, M.A.; Weiss, B. Ribosome pausing, a dangerous necessity for co-translational events. *Nucleic Acids Res.* **2020**, *48*, 1043–1055. [[CrossRef](#)]
85. Dever, T.E.; Dinman, J.D.; Green, R. Translation Elongation and Recoding in Eukaryotes. *Cold Spring Harb. Perspect. Biol.* **2018**, *10*, a032649. [[CrossRef](#)]

86. Tinoco, I., Jr.; Kim, H.K.; Yan, S. Frameshifting dynamics. *Biopolymers* **2013**, *99*, 1147–1166. [[CrossRef](#)]
87. Chong, J.L.; Chuang, R.Y.; Tung, L.; Chang, T.H. Ded1p, a conserved DExD/H-box translation factor, can promote yeast L-A virus negative-strand RNA synthesis in vitro. *Nucleic Acids Res.* **2004**, *32*, 2031–2038. [[CrossRef](#)] [[PubMed](#)]
88. Wickner, R.B. Double-stranded RNA viruses of *Saccharomyces cerevisiae*. *Microbiol. Rev.* **1996**, *60*, 250–265. [[CrossRef](#)]
89. Farabaugh, P.J. Programmed translational frameshifting. *Annu. Rev. Genet.* **1996**, *30*, 507–528. [[CrossRef](#)] [[PubMed](#)]
90. Itano, M.S.; Arnion, H.; Wolin, S.L.; Simon, S.M. Recruitment of 7SL RNA to assembling HIV-1 virus-like particles. *Traffic* **2018**, *19*, 36–43. [[CrossRef](#)]
91. Schmidt, M.O.; Brosh, R.M., Jr.; Oliver, D.B. *Escherichia coli* SecA helicase activity is not required in vivo for efficient protein translocation or autogenous regulation. *J. Biol. Chem.* **2001**, *276*, 37076–37085. [[CrossRef](#)] [[PubMed](#)]
92. Wang, S.; Jomaa, A.; Jaskolowski, M.; Yang, C.I.; Ban, N.; Shan, S.O. The molecular mechanism of cotranslational membrane protein recognition and targeting by SecA. *Nat. Struct. Mol. Biol.* **2019**, *26*, 919–929. [[CrossRef](#)] [[PubMed](#)]
93. Knüpfper, L.; Fehrenbach, C.; Denks, K.; Erichsen, V.; Petriman, N.A.; Koch, H.G. Molecular Mimicry of SecA and Signal Recognition Particle Binding to the Bacterial Ribosome. *mBio* **2019**, *10*, 1128. [[CrossRef](#)] [[PubMed](#)]
94. Tanner, N.K.; Cordin, O.; Banroques, J.; Doere, M.; Linder, P. The Q motif: A newly identified motif in DEAD box helicases may regulate ATP binding and hydrolysis. *Mol. Cell* **2003**, *11*, 127–138. [[CrossRef](#)] [[PubMed](#)]
95. de la Cruz, J.; Iost, I.; Kressler, D.; Linder, P. The p20 and Ded1 proteins have antagonistic roles in eIF4E-dependent translation in *Saccharomyces cerevisiae*. *Proc. Natl. Acad. Sci. USA* **1997**, *94*, 5201–5206. [[CrossRef](#)] [[PubMed](#)]
96. Janke, C.; Magiera, M.M.; Rathfelder, N.; Taxis, C.; Reber, S.; Maekawa, H.; Moreno-Borchart, A.; Doenges, G.; Schwob, E.; Schiebel, E.; et al. A versatile toolbox for PCR-based tagging of yeast genes: New fluorescent proteins, more markers and promoter substitution cassettes. *Yeast* **2004**, *21*, 947–962. [[CrossRef](#)] [[PubMed](#)]
97. Malcova, I.; Farkasovsky, M.; Senohrabkova, L.; Vasicova, P.; Hasek, J. New integrative modules for multicolor-protein labeling and live-cell imaging in *Saccharomyces cerevisiae*. *FEMS Yeast Res.* **2016**, *16*, fow027. [[CrossRef](#)] [[PubMed](#)]
98. Lin, R.J.; Newman, A.J.; Cheng, S.C.; Abelson, J. Yeast mRNA splicing in vitro. *J. Biol. Chem.* **1985**, *260*, 14780–14792. [[CrossRef](#)]
99. Guthrie, C.; Fink, G.R. (Eds.) *Guide to Yeast Genetics and Molecular Biology*; Academic Press: San Diego, CA, USA, 1991; Volume 194.
100. Carpousis, A.J.; Khemici, V.; Ait-Bara, S.; Poljak, L. Co-immunopurification of multiprotein complexes containing RNA-degrading enzymes. *Methods Enzymol.* **2008**, *447*, 65–82. [[CrossRef](#)]
101. Ream, J.A.; Lewis, L.K.; Lewis, K.A. Rapid agarose gel electrophoretic mobility shift assay for quantitating protein: RNA interactions. *Anal. Biochem.* **2016**, *511*, 36–41. [[CrossRef](#)]
102. Christiano, R.; Nagaraj, N.; Frohlich, F.; Walther, T.C. Global proteome turnover analyses of the Yeasts *S. cerevisiae* and *S. pombe*. *Cell Rep.* **2014**, *9*, 1959–1965. [[CrossRef](#)] [[PubMed](#)]

Disclaimer/Publisher’s Note: The statements, opinions and data contained in all publications are solely those of the individual author(s) and contributor(s) and not of MDPI and/or the editor(s). MDPI and/or the editor(s) disclaim responsibility for any injury to people or property resulting from any ideas, methods, instructions or products referred to in the content.